Pathology - Research and Practice 215 (2019) 177–194

Contents lists available at ScienceDirect

Pathology - Research and Practice

journal homepage: www.elsevier.com/locate/prp

Clinical and prognostic value of chaperonin containing T-complex 1 subunit 3 in hepatocellular carcinoma: A Study based on microarray and RNA-sequencing with 4272 cases

Jia-yin Hou[a], Hua-yu Wu[b], Rong-quan He[c], Peng Lin[d], Yi-wu Dang[a], Gang Chen[a,*]

[a] Department of Pathology, First Affiliated Hospital of Guangxi Medical University, Nanning, Guangxi Zhuang Autonomous Region 530021, China
[b] Department of Cell Biology and Genetics, School of Preclinical Medicine, Guangxi Medical University, Nanning, Guangxi Zhuang Autonomous Region 530021, China
[c] Department of Medical Oncology, First Affiliated Hospital of Guangxi Medical University, Nanning, Guangxi Zhuang Autonomous Region 530021, China
[d] Department of Ultrasonography, First Affiliated Hospital of Guangxi Medical University, Nanning, Guangxi Zhuang Autonomous Region 530021, China

ARTICLE INFO

Keywords:
Hepatocellular carcinoma
CCT3
DEGs
Prognosis
RNA sequencing
Clinicopathological parameters

ABSTRACT

Liver cancer is one of the few tumors with a steadily increasing morbidity and mortality; hepatocellular carcinoma (HCC) is the most common type of primary liver cancer. We combined the expression profiles of Chaperonin Containing T-complex 1 Subunit 3 (CCT3) in HCC tissues based on microarray and RNA-sequencing data. The CCT3 expression levels were extracted and examined based on 421 samples from The Cancer Genome Atlas (TCGA) (HCC, n = 371; non-HCC, n = 50) and 3851 samples from 31 microarray or RNA-sequencing datasets (HCC, n = 1975; non-tumor = 1876). We used a variety of meta-analytic methods, including SMD forest maps, sensitivity analysis, subgroup analysis and sROC curves, to confirm the final results. Meanwhile, database-derived immunohistochemistry data was used for validation. We also further explained the potential mechanism of CCT3 in HCC through signal pathway analyses and PPI network construction with the CCT3 co-expressed genes. The mRNA and protein expression of CCT3 in HCC tissues were higher than in non-HCC tissues. The expression of CCT3 differed between groups when grouped according to clinicopathological parameters, such as race, family history, and histological grade. The results of standardised mean difference (SMD) forest map and summary receiver operating characteristic (sROC) curve revealed that CCT3 was highly expressed in HCC tissues and had a high ability to distinguish between cancer tissues and non-cancer tissues. The main form of CCT3 gene alteration in HCC was mRNA up-regulation and amplification (23%), and the most common mutation type was missense. The mRNA expression of CCT3 in HCC was negatively correlated with DNA methylation. According to the Kyoto Encyclopedia of Genes and Genomes pathway analysis, CCT3 can influence HCC occurrence and development through cell cycle and DNA replication pathways. In summary, this study carries out the staging and prognostic analysis of HCC. It suggests that CCT3 might play an important part in the tumorigenesis and progression of HCC and may have a certain prognostic value in HCC. Moreover, CCT3 might represent a promising biomarker for HCC.

1. Introduction

Liver cancer is one of the few tumors with a steadily increasing morbidity and mortality. Hepatocellular carcinoma (HCC) is the most common type of primary liver cancer, accounting for 90% of all cases of liver cancer; nearly 800 thousand new cases are reported each year [1,2]. HCC is the leading cause of cancer deaths worldwide, due to the high incidence of chronic hepatitis B(HBV) infection. Liver cancer is prevalent mainly in Asia and Africa [3,4]. In the early stage of HCC, some surgical procedures, such as surgical resection, liver transplantation, and local ablation, can improve patients' survival rate. However, when HCC is discovered at a late stage, the available therapies are limited to palliative and local treatments. Therefore, the early detection of HCC is essential for improving patients' survival rate and quality of life [5,6]. Our understanding of the molecular mechanism of HCC has significantly

* Corresponding author at: Department of Pathology, First Affiliated Hospital of Guangxi Medical University, No. 6. Shuangyong Rd., Nanning, Guangxi Zhuang Autonomous Region, 530021, China.
E-mail address: chengang@gxmu.edu.cn (G. Chen).

https://doi.org/10.1016/j.prp.2018.11.006
Received 28 July 2018; Received in revised form 25 October 2018; Accepted 6 November 2018

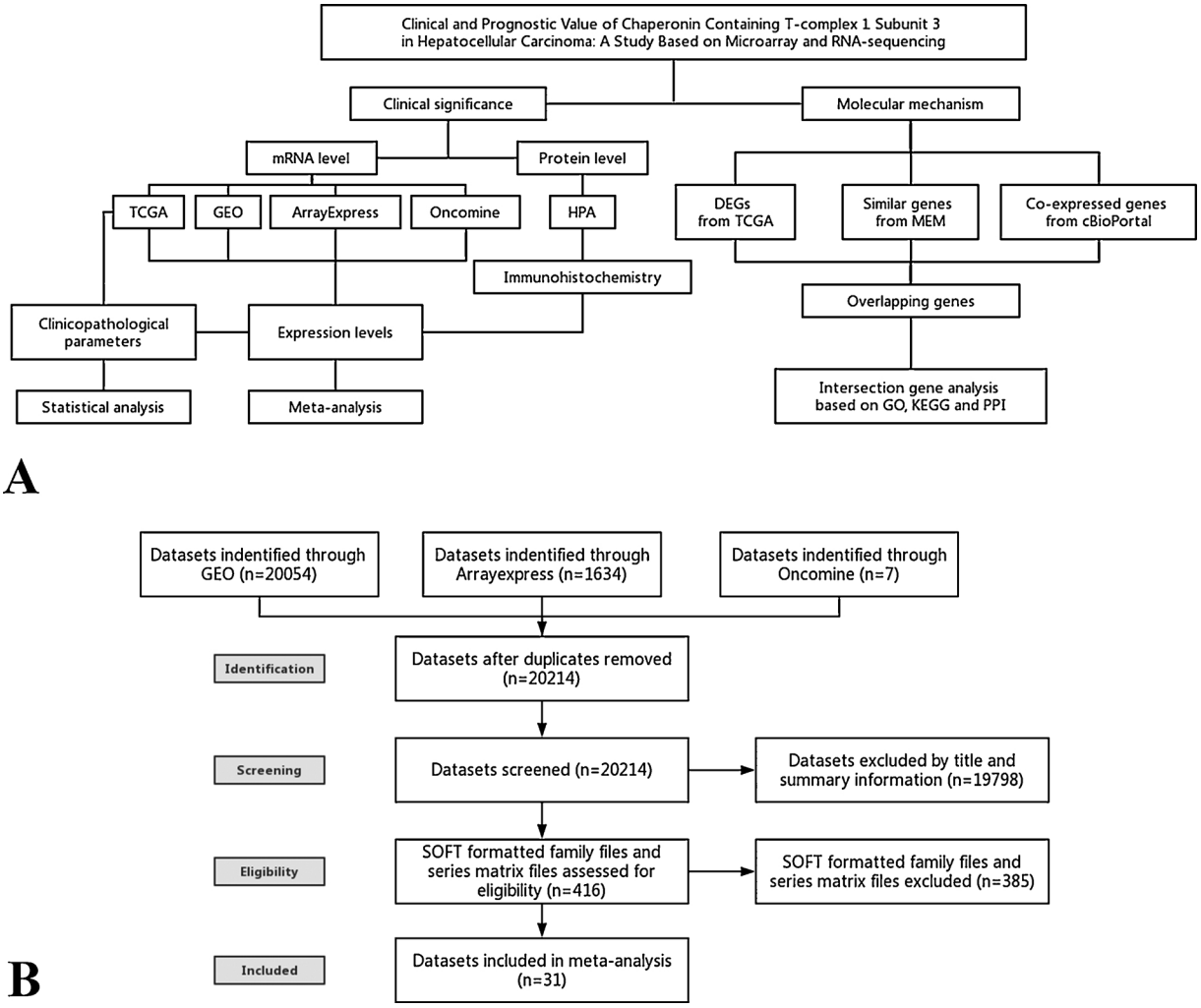

Fig. 1. Flow charts. (A)Flow chart of the study design; (B) Flow chart of the study search and selection.

improved in the past decade due to the accumulation of data from high-throughput analyses of a large number of samples. As a result, we are able to delineate some key events that may be related to tumorigenesis and progression, thereby discovering new targets and biomarkers that can improve the prognosis of HCC patients [7–12].

The t-complex 1 (TCP1) loop complex (TRiC) can act as a molecular chaperone that participates in actin and tubulin folding. When TCP1 was first discovered, it was found to be a protein coded by a gene locus on mouse chromosome 17, which was related to several genetic defects. In humans, TCP1 is a 60 kD subunit of the cytoplasmic hetero-oligomeric chaperone. This protein belongs to the family of chaperone proteins that assist in the folding of proteins when ATP is hydrolyzed. The human TRiC-P5 gene (TRIC5/CCT3) is located on human chromosome lq23. CCT3 has significant sequence similarity with other members of the CCT family of chaperone proteins and shares conserved domains with other distant chaperone proteins [13,14].

Earlier studies found that CCT3 was differentially expressed in the HCC and non-tumor control samples, and the expression of CCT3 was correlated with overall survival rate [15–17]. The expression of CCT3 in the plasma samples of HCC patients, liver cirrhosis patients, and healthy volunteers was detected by enzyme-linked immunosorbent assay. The expression of CCT3 in HCC patients was found to be significantly higher than in liver cirrhosis patients and healthy volunteers; the differing expression was associated with a variety of clinicopathological parameters. The detection of CCT3 content can complement the screening and diagnosis of α-fetoprotein negative HCC patients [17]. Moreover, several studies have also explored the role and molecular mechanisms of CCT3 in the tumorigenesis and progression of HCC. A study conducted by Cui et al. (2015) found that mRNA and protein levels of CCT3 were significantly up-regulated in tumor tissues compared with non-tumor tissues, and the down-regulation of CCT3 may be correlated with prognosis. Through polymerase chain reaction (PCR) and a variety of experiments, they found down-regulation of CCT3 can inhibit the invasive ability of HCC cells, and CCT3 might act as a novel target of STAT3 activation in HCC patients [18]. Similarly, in a study conducted by Zhang, et al. (2015), researchers also found that CCT3 consumption can inhibit the proliferation of HCC cells by inducing mitotic arrest in the early-middle stages and eventually inducing apoptosis. Therefore, CCT3 plays an important role in the proliferation of HCC cells and provides a potential therapeutic target for clinical drug research with regard to HCC [19].

Given the above findings, we searched several public databases to obtain the expression profile of CCT3 in HCC and corresponding control tissues. We then used meta-analysis and bioinformatics to verify the clinical and prognostic value of CCT3 in HCC and conduct more in-depth studies.

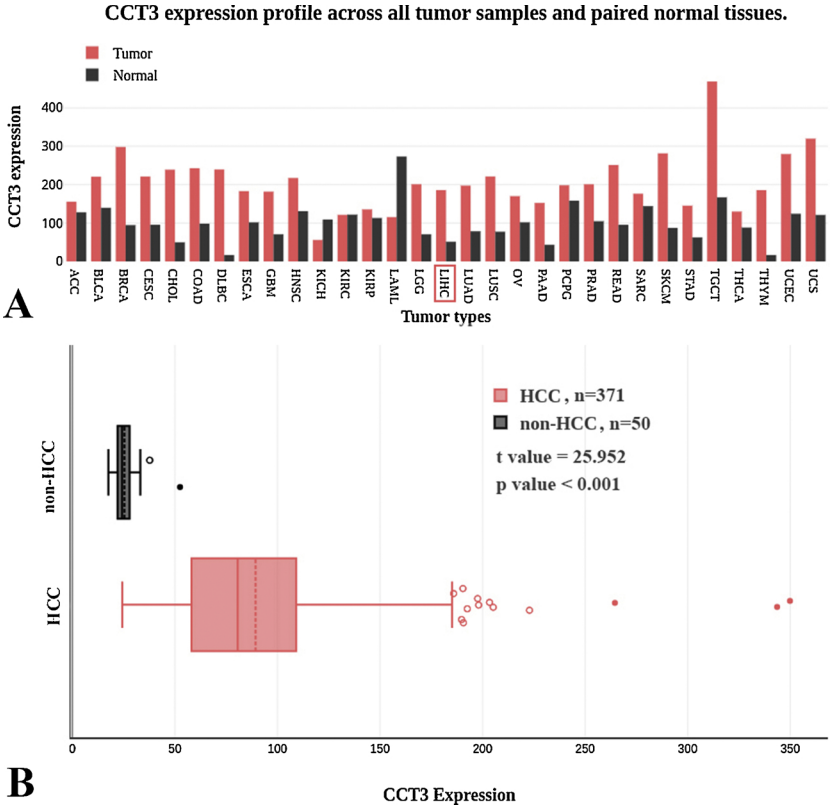

Fig. 2. CCT3 expression pattern from The Cancer Genome Atlas (TCGA). (A) Expression levels of CCT3 are presented based on Gene Expression Profiling Interactive Analysis (GEPIA). The height of bar represents the median expression of certain tumor type or normal tissue(ACC: Adrenocortical carcinoma, BLCA: Bladder Urothelial Carcinoma, BRCA: Breast invasive carcinoma, CESC: Cervical squamous cell carcinoma and endocervical adenocarcinoma, CHOL: Cholangiocarcinoma, COAD: Colon adenocarcinoma, DLBC: Lymphoid Neoplasm Diffuse Large B-cell Lymphoma, ESCA: Esophageal carcinoma, GBM: Glioblastoma multiforme, HNSC: Head and Neck squamous cell carcinoma, KICH: Kidney Chromophobe, KIRC: Kidney renal clear cell carcinoma, KIRP: Kidney renal papillary cell carcinoma, LAML: Acute Myeloid Leukemia, LGG: Brain Lower Grade Glioma, LIHC: Liver hepatocellular carcinoma, LUAD: Lung adenocarcinoma, LUSC: Lung squamous cell carcinoma, OV: Ovarian serous cystadenocarcinoma, PAAD: Pancreatic adenocarcinoma, PCPG: Pheochromocytoma and Paraganglioma, PRAD: Prostate adenocarcinoma, READ:Rectum adenocarcinoma, SARC: Sarcoma, SKCM: Skin Cutaneous Melanoma, STAD: Stomach adenocarcinoma, TGCT: Testicular Germ Cell Tumors, THCA: Thyroid carcinoma, THYM: Thymoma, UCEC: Uterine Corpus Endometrial Carcinoma, UCS: Uterine Carcinosarcoma.); (B) Box chart of CCT3 expression in HCC and non-HCC liver tissues. Expression of CCT3 was significantly higher in HCC tissue, based on the TCGA database (HCC tissue: 89.320 ± 44.98, control tissue: 25.390 ± 5.54, t value: 25.952, $p < 0.001$). (CCT3 expression represent the relative expression preprocessed by log-2 transformation.).

2. Materials and methods

2.1. Data sources

2.1.1. TCGA database

The expression data and clinicopathological parameters of CCT3 in HCC from the The Cancer Genome Atlas (TCGA) database were analyzed, including 371 HCC samples and 50 non-tumor control samples. The expression data is log-2 transformed level3 RNA-seq data. We downloaded the read counts and the FPKM-UQ data separately for different subsequent processing. The clinicopathological parameters included age, race, gender, race, family history, Child-Pugh class, new tumor event after initial treatment, histological grade, pathological stage, and TNM stage.

2.1.2. Other public databases

We searched the Group on Earth Observations (GEO) database to obtain the expression data and related clinical parameters of CCT3 in HCC tissues and control tissues. The search formula was as follows: (hepatocellular OR liver OR hepatic* OR HCC) AND (carcinoma OR cancer OR tumor OR neoplas* OR malignan*). The selected conditions were: (1) the species is human; (2) sample type is tissue; (3) microarray and high-throughput sequencing results containing the desired gene; and (4) containing HCC tissue and non-tumor tissue controls. The excluded conditions were: (1) control samples have other non-study related disease effects ; and (2) containing drug-related research and other unrelated interventions. The first author, publication year, country, platform, and CCT3 expression data were extracted from the screened results. All the screening and extraction procedures were independently performed and compared by two investigators. When the results were inconsistent, a third investigator reviewed them, and the three investigators discussed them to reach consensus.

We downloaded the expression data of CCT3 in HCC and non-HCC control tissues from the Oncomine and ArrayExpress databases. The processing of all chips is as follows. All the datasets are collected from different platforms, including Affymetrix, Illumina, Rosetta, CapitalBio, Agilent, Arraystar and NimbleGen, the mRNA expression have been normalized signal intensities using Intensity-dependent normalization. Value distribution, an useful function provide by GEO database, is a box plot showing the distribution of expression level of each sample within a dataset which would determine whether the dataset is normalized. We used this function to check the standardization status of each chip before it was downloaded. And after downloading the chips, we have performed log-2 transformation and use the sva package (http://bioconductor.org/packages/sva/) based on R language to remove the batch effect. The flow chart of the study search and selection was as follows [Fig. 1B].

2.2. Data processing

2.2.1. Data processing in the TCGA database

We used SPSS 24.0 (SPSS Inc., Chicago, IL, USA) to calculate the expression of CCT3 in HCC tissues and non-tumor control tissues. The mean and standard deviations were used to indicate their expression levels. Two Independent Samples t-tests were used to compare the expression of CCT3 in the two groups of samples. Differing expressions of CCT3 between clinicopathological parameters such as age, family history, gender, Child-Pugh class, new tumor event after initial treatment, neoplasm cancer status, histological grade, pathological stage, and TNM staging were compared. A chi-square test was used to compare differences in CCT3 expression among races. Box plots drawn by GraphPad Prism 5 (San Diego, CA, USA) show differences in the expression of CCT3 among different clinicopathological parameters. We determined a p-value of less than 0.05 to be a statistically significant cut-off.

Table 1
The mean and standard deviation of CCT3 expression values in HCC and non-HCC tissues, based on 36 GEO chips, one ArrayExpress chip and three Oncomine chips. (N represents the total number of tissue samples, Mean represents average expression level, and SD represents standard deviation, respectively).

Author	Publication year	Country	Dataset	Data type	Platform	Cancer			Non-tumor		
						N	Mean	SD	N	Mean	SD
Hoshida	10 January 2008	USA	GSE10143	Microarray	Illumina GPL5474	80	14.5478	0.2240	307	13.4725	0.4847
Yamada	26 September 2008	Japan	GSE12941	Microarray	Affymetrix GPL5175	10	9.3141	0.3373	10	8.2552	0.2447
Mas	07 January 2009	USA	GSE14323	Microarray	Affymetrix GPL96/GPL571	64	9.4371	0.5889	60	9.3512	0.3202
Burchard	30 May 2010	USA	GSE22058	Microarray	Affymetrix GPL6793	100	13.0113	0.3759	97	12.2595	0.1910
Zhang	17 June 2010	USA	GSE22405	Microarray	Affymetrix GPL10553	24	8.6509	1.2759	24	7.0064	1.1549
Zhang	03 November 2010	USA	GSE25097	Microarray	Rosetta GPL10687	268	14.5255	4.4466	289	8.5373	1.3648
Xing	24 November 2010	USA	GSE25599	Sequencing	Illumina GPL9052	10	6.9392	0.8966	10	5.5045	0.3462
Park	08 March 2012	South Korea	GSE36376	Microarray	Illumina GPL10558	240	9.4148	0.5369	193	8.1306	0.2013
Kim	31 July 2012	USA	GSE39791	Microarray	Illumina GPL10558	72	9.4402	0.6191	72	8.4924	0.2840
Wei	12 March 2013	China	GSE45114	Microarray	CapitalBio GPL5918	24	1.4065	0.8166	25	0.0344	0.5254
Jeng	26 Apr 2013	China (Taiwan)	GSE46408	Microarray	Agilent GPL4133	6	13.8777	0.9349	6	12.3598	0.3195
Geffers	04 September 2013	Germany	GSE50579	Microarray	Agilent GPL14550	67	13.3943	0.6930	13	12.7016	1.2603
Villa	21 January 2014	Italy	GSE54236	Microarray	Agilent GPL6480	81	13.9114	0.6542	80	13.2694	0.4261
Yuan	21 January 2014	USA	GSE54238	Microarray	Arraystar GPL16955	26	13.1397	0.7736	30	11.7531	0.3502
Melis	18 February 2014	USA	GSE55092	Microarray	Affymetrix GPL570	49	10.6333	0.8877	91	9.6101	0.5651
Hoshida	24 March 2014	New York	GSE56140	Microarray	Illumina GPL18461	35	7.9484	0.3410	34	7.3086	0.2380
Mah	24 May 2014	USA	GSE57957	Microarray	Illumina GPL10558	39	10.7120	0.5680	39	9.8545	0.2448
Udali	09 July 2014	Italy	GSE59259	Microarray	NimbleGen GPL18451	8	13.2733	0.6006	8	12.7791	0.2022
Kao	18 August 2014	China (Taiwan)	GSE60502	Microarray	Affymetrix GPL96	18	11.7787	0.5918	18	10.7335	0.2730
Zucman-Rossi	09 October 2014	France	GSE62232	Microarray	Affymetrix GPL570	81	10.3544	0.5751	10	9.0565	0.2166
Makowska	10 December 2014	USA	GSE64041	Microarray	Affymetrix GPL6244	120	9.1821	0.4986	5	8.7931	0.1491
Tao	03 November 2015	China	GSE74656	Microarray	Affymetrix GPL16043	5	11.0764	0.5150	5	9.9072	0.1830
Grinchuk	30 December 2015	Singapore	GSE76427	Microarray	Illumina GPL10558	115	10.7078	0.4900	52	10.0425	0.2570
Jin	02 February 2016	China	GSE77509	Sequencing	Illumina GPL16791	20	14.8048	0.6002	20	13.1486	0.2590
Tu	05 July 2016	China	GSE84005	Microarray	Affymetrix GPL5175	38	9.7826	0.6357	38	8.6332	0.2460
Qin	14 July 2016	China	GSE84402	Microarray	Affymetrix GPL570	14	9.8895	1.1231	14	8.5119	0.8128
Woo	05 October 2016	South Korea	GSE87630	Microarray	Illumina GPL6947	64	3.4707	0.0849	30	3.2853	0.0495
Nojima	01 April 2017	Japan	E-MTAB-4171	Microarray	Agilent A-MEXP-2320	15	15.5897	0.6252	15	14.2874	0.2395
Wurmbach	21 June 2007	USA	Wurmbach Liver	Microarray	Affymetrix GPL570	35	11.6133	0.7298	40	10.2209	0.3430
Roessler	01 December 2010	USA	Roessler Liver	Microarray	Affymetrix GPL571	22	9.7711	0.4837	21	8.1828	0.3664
Roessler	01 December 2010	USA	Roessler Liver 2	Microarray	Affymetrix GPL3921	225	9.5865	0.6356	220	8.0168	0.3882

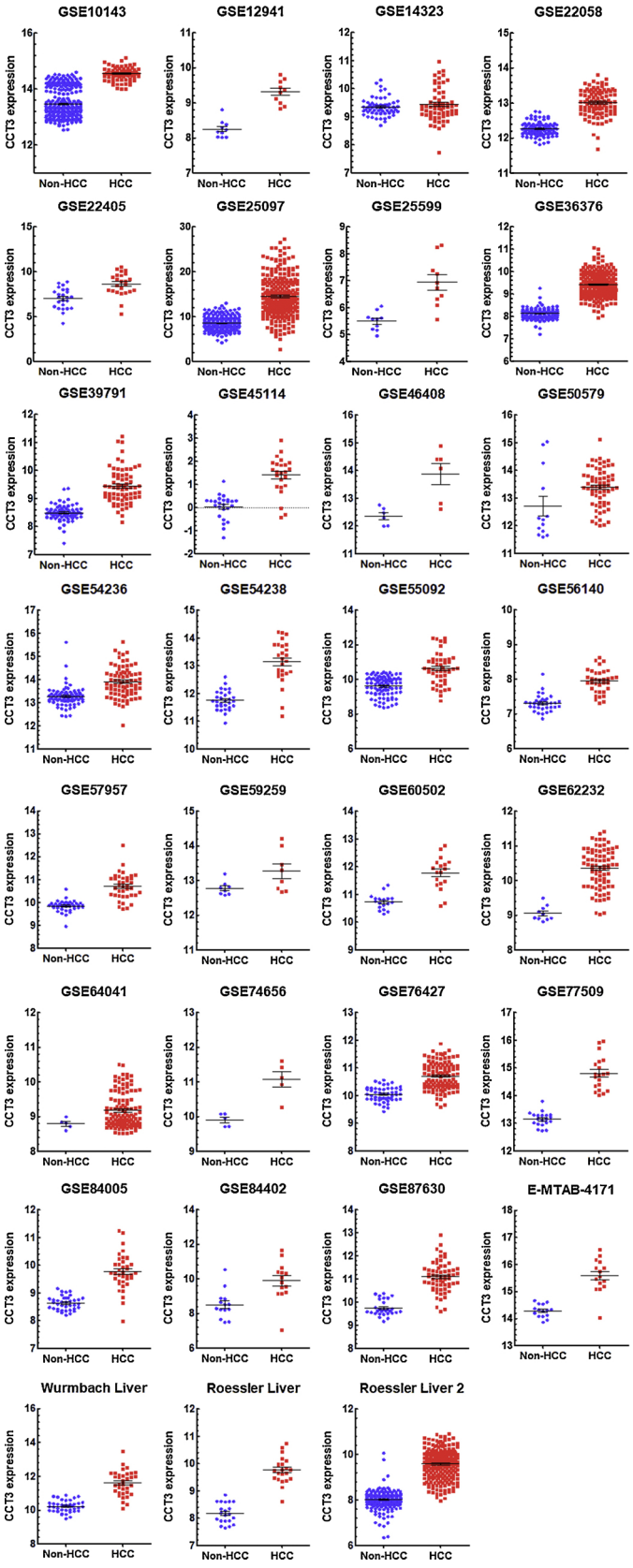

Fig. 3. Different expression levels of CCT3 in HCC and non-HCC tissues based on 31 datasets. GraphPad Prism5 was used to draw scatter plots to visualize the results. Among all the 31 chips, CCT3 showed high expression in cancer tissues. (CCT3 expression represent the relative expression preprocessed by log-2 transformation).

2.2.2. Data processing of other public databases

We extracted the expression of CCT3 from various chips obtained from GEO, Oncomine, and ArrayExpress. We performed log2 standardization on unstandardized data and used SPSS 24.0 to calculate the mean and standard deviation of CCT3 expression in HCC tissues and non-tumor tissues. GraphPad Prism5 was used to draw scatter plots and receiver operating characteristic (ROC) curves to visualize the results. We used STATA 12.0 (StataCorp, College Station, TX, USA) for meta-analysis and drew SMD forest maps. When the SMD was greater than 0 and its 95% confidence interval did not intersect with ineffective lines, the expression of CCT3 was considered to be significantly higher in cancer tissues. We also calculated the yonder index by using SPSS 24.0 to plot the ROC curve results. The cut-off value was derived according to the Youden index. The number of cancerous samples above the cut-off value was taken as the number of true positives, and the number of non-cancerous samples above the cut-off value was taken as the number of false positives. The area under the curve (AUC) and its 95% confidence interval were calculated. The summary ROC (SROC) curve was plotted and used as a visual statistical method; by calculating the AUC of the SROC curve, we studied the differences in the expression of CCT3 between tumor and non-tumor tissues.

2.2.3. Immunohistochemistry

The Human Protein Atlas (HPA) is a program mapped all the human proteins in cells, tissues and organs. It contains the expression profiles of human genes on the protein level derived from immunohistochemistry. All images of immunohistochemistry stained tissues are available in this program. We used this database to validate the differential protein expression of CCT3 between HCC tissues and non-cancer tissues.

The results of immunohistochemical staining were mainly based on the HPA website, and the interpretation criteria were determined according to the actual situation. The interpretation standards can be described in the following manner: first, results were scored according to staining intensity (I)— staining low is 1 point, staining medium is 2 points, staining high is 3 points; then, results were scored according to the percentages (P) that positive cells occupy— $< 25\%$ is 1 point, $25\% \sim 75\%$ is 2 points, $> 75\%$ is 3 points; lastly, the two numbers were multiplied to obtain (Q), that is, $Q = P \times I$. When the score is $Q < 4$, it is considered negative; when the score is $Q \geq 4$, it is considered positive [20].

2.3. Study on gene alteration and mutation types

The raw data from the cBio Cancer Genomics Portal (cBioPortal) comes from several databases, which enable researchers to query the alteration of each gene, and analyze genomic and clinical data. We selected the appropriate data set (TCGA) in the cBioPortal database to verificate the gene changes in CCT3, including mutation, genotype analysis, and gene loci. The cBioPortal database can compute the relative expression value of an individual gene distribution in a reference population(population that all samples that are diploid for the target gene, or normal samples, or all profiled samples). The returned value, Z-score indicates the value of standard deviations away from the mean of mRNA expression in this reference population. This measurement can be used to determine whether the expression level of a certain gene is up- or down-regulated relative to a normal sample or tumor sample.The z-score data is essential for the OncoPrints functionality which could visualize different genomic changes, including copy number changes, somatic mutations, and changes in mRNA expression in a group of cases. The oncoprint can show over- and under-expression of the data, based on the threshold the user sets when selecting the genomic profile. Herein, we set the

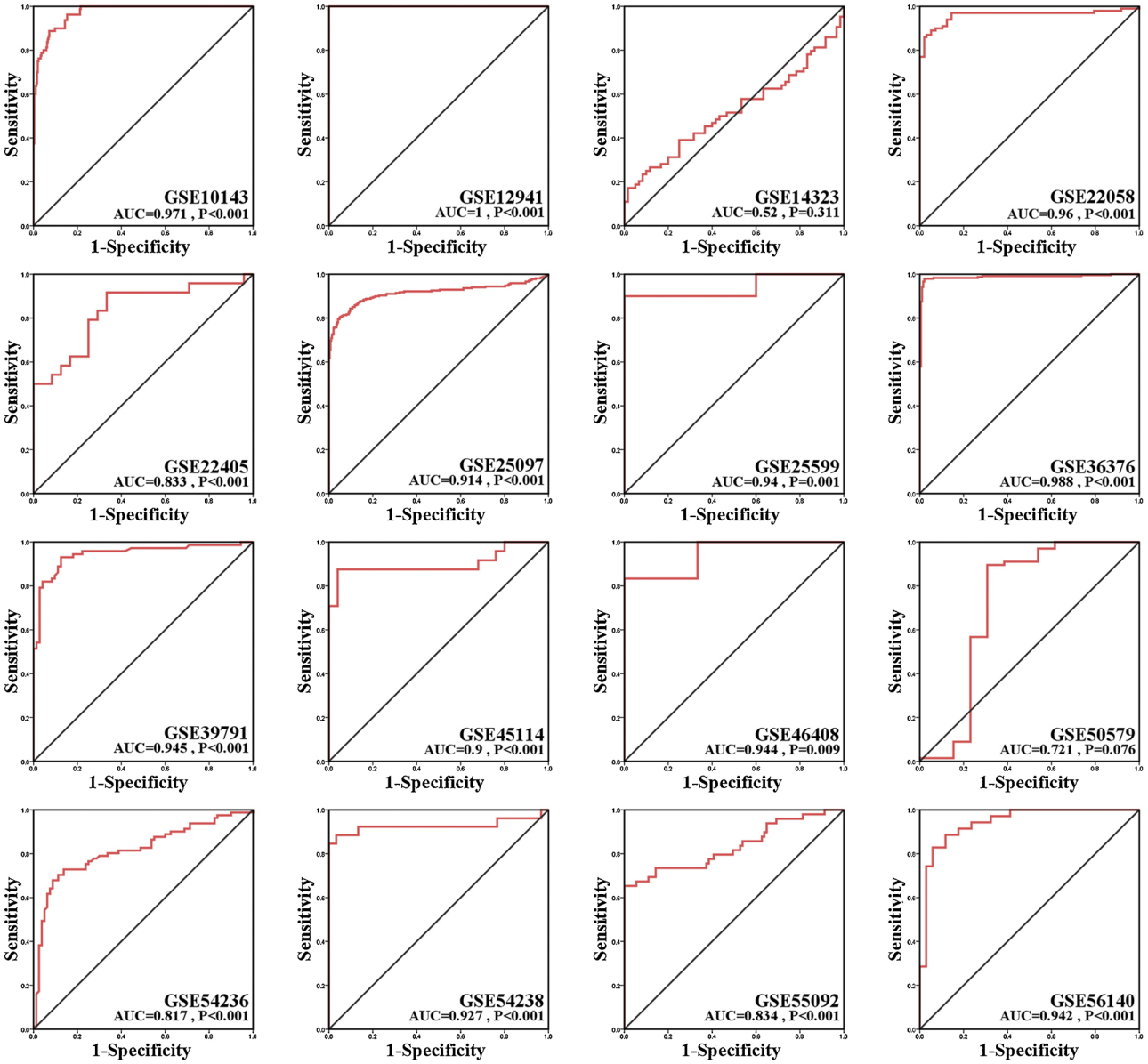

Fig. 4. ROC curves of the differential expression of CCT3 in non-HCC and HCC tissues, based on 31 datasets. (AUC: area under curve.) GraphPad Prism5 was used to draw ROC curves to visualize the results. Among all the 31 chips, CCT3 showed a high ability to distinguish between cancer and non-cancer tissues.

z-score threshold as ± 2.0, The "cases with alteration" are patients with high expression of CCT3 and the cases without alteration are those with low expression of CCT3. It is worth noting that the z-scores are calculated using only patient data. Hence, over-expressed in this case implies higher expression than the average patient. Therefore, when using independent sample *t*-test to analyze cancer and non-cancer samples from TCGA, CCT3 may show a significantly higher expression trend, at the same time, difference of CCT3 expression in cBioPortal was not particularly significant. In addition, a similarity analysis was conducted on 440 HCC samples collected from TCGA database (as of August 7, 2018) using this database and the relevant survival curves were drawn on the basis of the prognosis time of cases with CCT3 genetic alteration in TCGA database. The cBioPortal database also provided a centralized set of different ways to visualize discrete genetic events (CNA or mutations) and continuous events, such as DNA methylation data. A number of studies have confirmed that DNA methylation played an important role in tumor development, risk prediction and drug combination therapy, so we also explored the association between mRNA expression of CCT3 and DNA methylation. The Catalogue of Somatic Mutations in Cancer (COSMIC) is a large and comprehensive dataset for exploring the effect of genetic mutations in human cancer. The COSMIC database combines two main types of data: high precision data curated by experts, and genome-wide screen data.Together, this compilation of data provides extensive coverage of the cancer genomic landscape from a somatic perspective. COSMIC makes it possible to study the common mutation types of CCT3 in HCC.

2.4. Bioinformatics analysis

We used the edgeR package, based on the R language [22], to analyze the RNA-sequencing files downloaded from TCGA. We set fold change = 1 and padj = 0.05 to find differentially expressed genes in HCC tumor tissues and non-tumor control tissues. We used

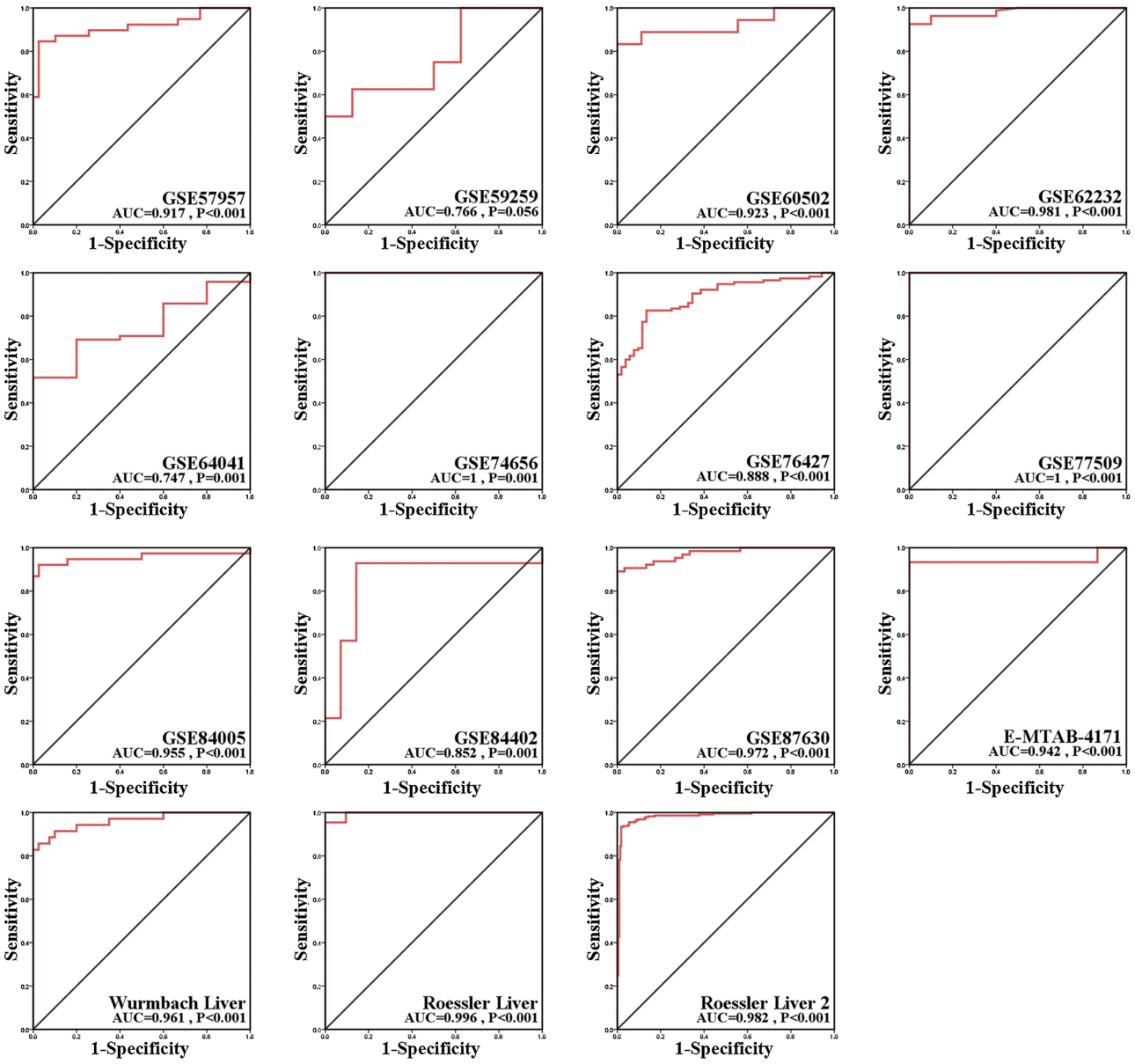

Fig. 4. (*continued*)

the Multi Experiment Matrix (MEM) website to find similar genes for CCT3, and then used the cBioPortal database to look for CCT3 co-expressed genes; we then cross-linked the resulting genes. The intersection genes were taken at the intersection with the previously obtained, differentially expressed gene, and all the genes related to the research target were obtained as accurately as possible. The overlapping genes were analyzed according to the Gene Ontology (GO) and Kyoto Encyclopedia of Genes and Genomes (KEGG) pathways using the WEB-based Gene SeT AnaLysis Toolkit (WebGestalt) database. The significance level was set to FDR < 0.05. We also used intersection genes that were enriched on the top five GO and KEGG pathways to map a protein–protein interaction network by STRING website. The thickness of the lines between two nodes indicated the strength of research support and the minimum confidence interaction score was set to the highest confidence (0.900).

The flow chart of the study design was as follows [Fig. 1A].

3. Results

3.1. Data processing

3.1.1. Analysis of CCT3 expression in the TCGA database

The Gene Expression Profiling Interactive Analysis (GEPIA) database was consulted to determine the expression of CCT3 in various cancers. CCT3 was found to be highly expressed in 28 types of cancer, including HCC [Fig. 2A]. Gene expression FPKM data for HCC and non-HCC controls were downloaded from the TCGA database. FPKM data wass converted to TPM data using R language, which removed the effect of sequencing depth and gene length on expression levels [21]. After log-2 transforming (the formula is: log2(TPM + 1)) and calculation, the expression of CCT3 in HCC tissues was significantly higher

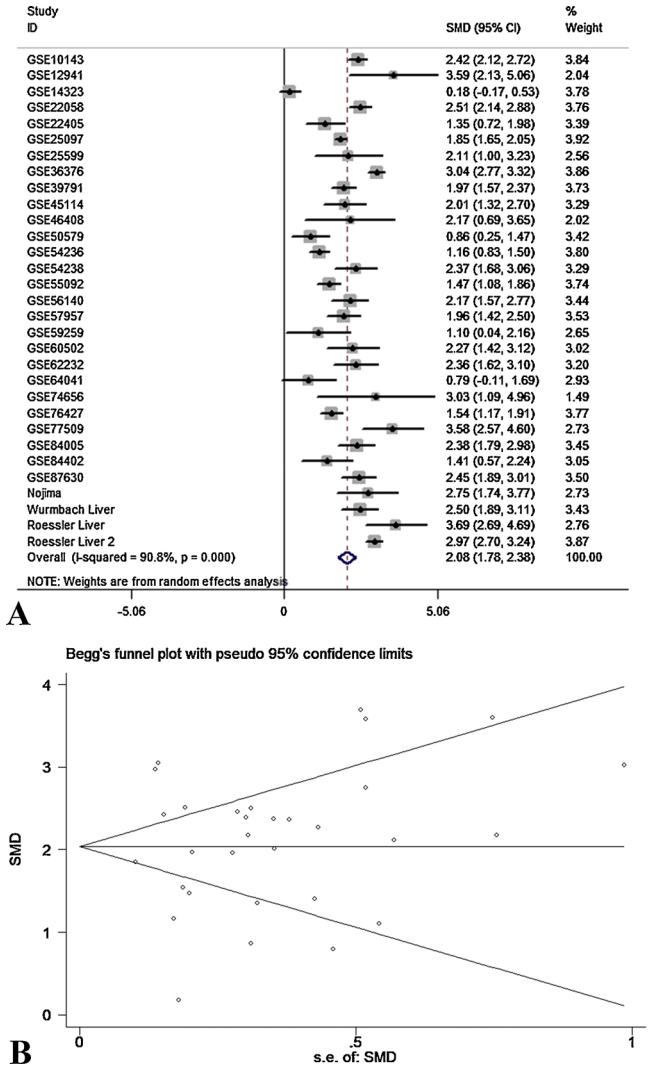

Fig. 5. Forest plot and Begg's funnel plot evaluating CCT3 expression between HCC and non-HCC tissues. (A) Because of the heterogeneity, a random effect model was used (I2 = 92.9%, p = 0.000). When the SMD was greater than 0 and its 95% confidence interval did not intersect with ineffective lines, the expression of CCT3 was considered to be significantly higher in cancer tissues (z = 13.64, p < 0.001); (B) Begg's funnel plot of SMD. The plot was drown by Metabias command. The publication bias was not significant (P = 0.892).

than in non-HCC tissues (p < 0.001) [Fig. 2B].

3.2. Analysis of CCT3 expression in other public databases

A total of 27 GEO chips, one ArrayExpress chip and three Oncomine chips were searched and screened, and the mean and standard deviation of CCT3 expression values in HCC and non-HCC tissues were calculated, respectively [Table 1]. Among all the 31 chips, CCT3 showed high expression in cancer tissues. To visualize the differences in the expression of CCT3 between cancer tissues and non-cancer tissues, scatter plots and ROC curves were plotted [Figs. 3 and 4]. The expression level of CCT3 in all studies was analyzed by SMD merging, and the forest map was drawn. It can be considered that the expression of CCT3 in cancer tissues was generally higher than that of non-cancer tissues (z = 13.64, p < 0.001) [Fig. 5A].The begg's funnel plot showed no publication bias in our analysis [Fig. 5B]. In the figures related to meta analysis, each dot represented a chip or dataset in this study. To study the use of CCT3 expression to distinguish between cancer tissue and non-cancer tissue, a meta-analysis was conducted to draw an SROC curve [Fig. 6A]. Funnel plot, as well as the forest plots of estimated sensitivity and specificity were also drawn. The results showed sensitivity and specificity are highly heterogeneous, and there was no public bias in our study [Fig. 6B, C, D].

In addition, to elucidate whether any single study was responsible for heterogeneity, a sensitivity analysis was performed by STATA 12.0 [Fig. 7]. No individual study contributed predominantly to heterogeneity according to the sensitivity analysis. Considering that multiple factors also might cause heterogeneity, subgroup analysis was conducted based on control tissue type, and the living region of patients. The results of this subgroup analysis are shown in Table 2, [Fig. 8].

3.2.1. Immunohistochemistry

The HPA database was used to validate the protein expression of CCT3, we collected the patient information and immunohistochemistry results from the website [Table 3] and conducted the Chi-square test [Table 4]. As the following figures indicate, the protein expression of CCT3 is significantly higher in the HCC tissues than in the non-cancer liver tissues [Fig. 9].

1.1.4Analysis of the Relationship between CCT3 Expression and Clinicopathological Parameters, based on the TCGA Database

The analysis of the data provided by the TCGA database indicated significant differences in the expression of CCT3 in various clinicopathological parameters, such as race, family history, histological grade, and TNM stage [Table 5]. The expression of CCT3 was found to be statistically different among three races. After a pairwise comparison using an SLD-t test, we see the expression of CCT3 in people of Asian descent was higher than that of Caucasians. There was no significant difference in the expression of CCT3 between Asians and Africans, or between Caucasians and Africans. This is probably due to the fact that the number of samples of Africans is much lower than those of Caucasians and Asians. In addition, there was no evidence to show that HCC patients of different age, sex, Child-Pugh class, new tumor event after initial treatment, neoplasm cancer status, pathological stage, or TNM stage had a differential expression of CCT3 [Fig. 10].

Moreover, survival curves were drawn by the GEPIA website, based on the TCGA survival data; cut-off value was selected as the median of CCT3 expression. The overall survival curve indicates that patients with a high expression of CCT3 were more likely to have a worse prognosis than those with a low expression of CCT3. We did not reach a similar conclusion with regard to the disease-free survival curve, but the two curves show a certain trend of separation; however, it is necessary to expand the sample size for further study [Fig. 11A, B]. At the same time, it is not surprising that the data from cBioPortal database provided a similar result based on the patients with or without CCT3 gene alteration. Patients with CCT3 amplification and mRNA up-regulation had poor overall survival. This result is also consistent with the effect of differential expression of CCT3 on patient outcomes [Fig. 11C, D].

3.3. Gene alteration and mutation types

Following analysis of the gene changes in CCT3 in TCGA datasets using the cBioPortal database, we found that the main form of gene alteration is mRNA up-regulation and amplification. The schematic of OncoPrint was produced for visualizing the alterations directly in HCC from cBioPortal. Gene amplification can affect transcription level, which likely eventually lead to the up-regulation of mRNA. Nevertheless, this hypothesis still needs experimental validation [Fig. 12A]. This result is also consistent with the differential mRNA expression of CCT3 in the TCGA database and several other gene chips. The mutation types of CCT3 in HCC were analyzed by the COSMIC database; the results are shown in Table 6. The methylation result

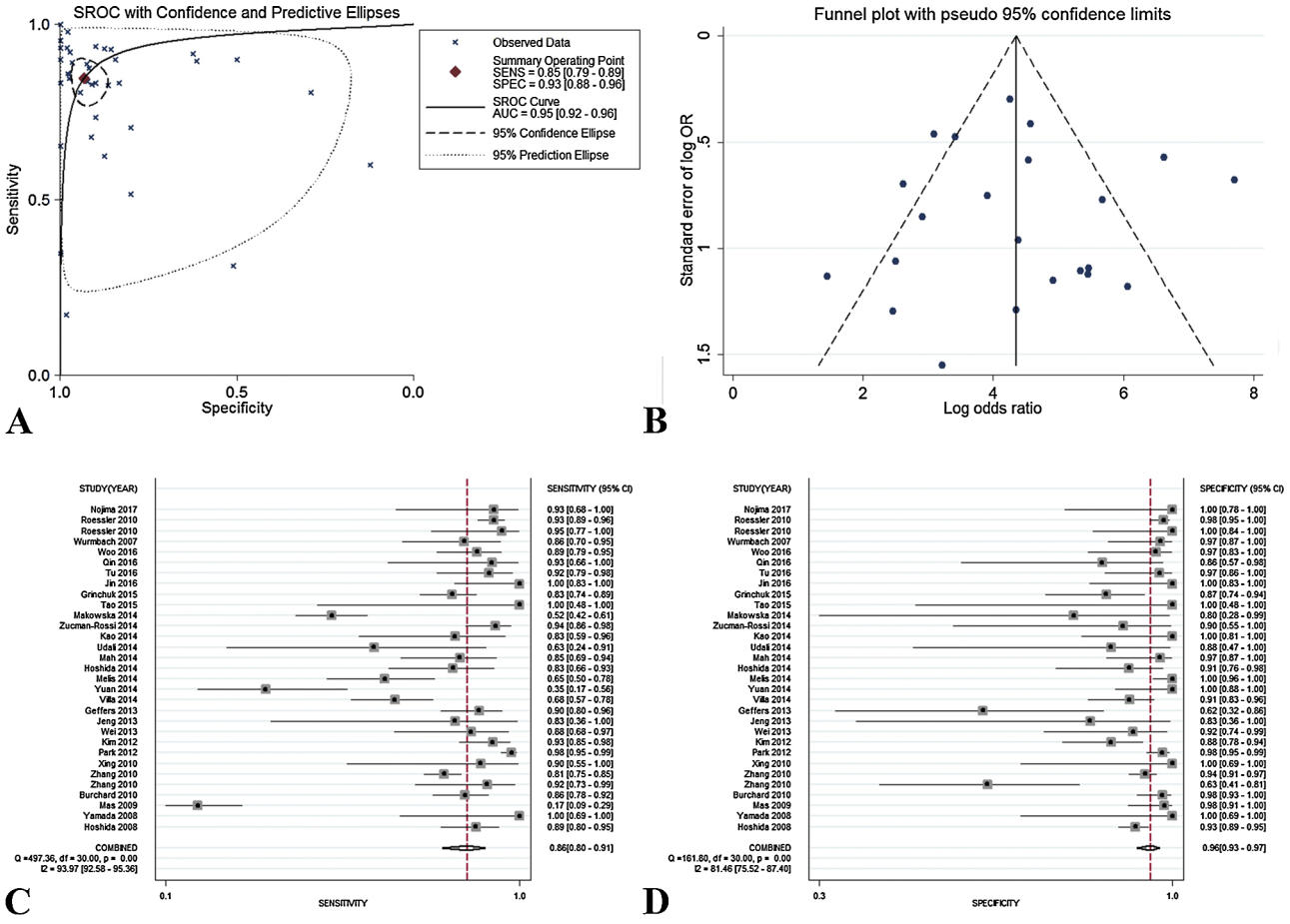

Fig. 6. The results of meta-analysis. SROC curves for the differentiation of HCC patients from non-HCC tissues based on CCT3 expression. The AUC was 0.95, which indicated that the expression of CCT3 had a high ability to distinguish cancer tissue from non-cancer tissue; (B) Diagnostic experiment funnel plot with pseudo 95% confidence limits. The plot was drown by Funnel command. The publication bias was not significant (Begg's test: P = 1.000; Egger's test: P = 0.949.); (C) Forest plot of estimated sensitivity; (D) Forest plot of estimated specificity.

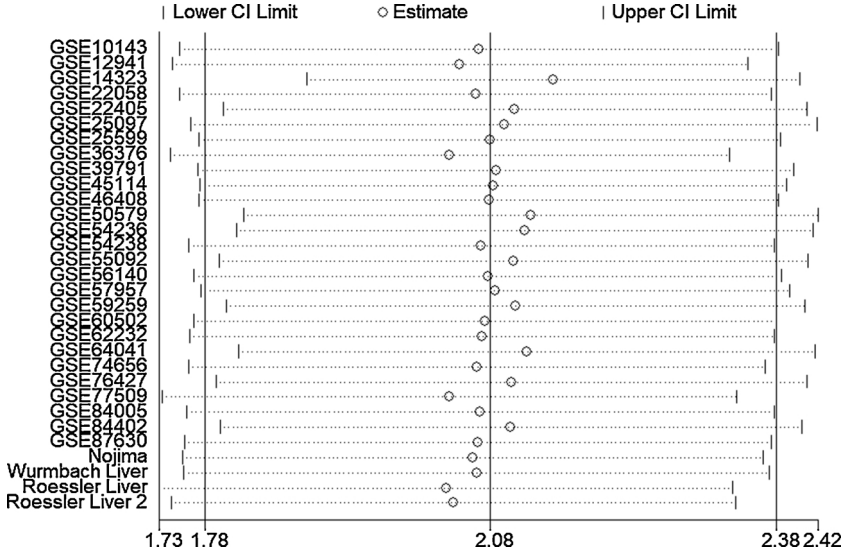

Fig. 7. The result of sensitivity analysis. The sensitivity analysis showed no individual study contributed predominantly to heterogeneity. Each hollow dot represents a chip or dataset in this study.

Table 2
Subgroup analyses for CCT3 differential expression between different type of HCC patients.

Subgroups		Number of studies	Pooled value		Heterogeneity statistic	
			SMD(95%CI)	p	I^2	p
Control tissue type	Cirrhotic liver tissues	5	1.70(0.76-2.64)	< 0.001	95.9	< 0.001
	Tumor adjacent liver tissues	21	2.09(1.79-2.39)	< 0.001	85.1	< 0.001
	Normal liver tissues	8	2.11(1.42-2.79)	< 0.001	89.1	< 0.001
Region	North America	15	2.01(1.59-2.43)	< 0.001	83.0	< 0.001
	Asia	12	2.44(1.99-2.89)	< 0.001	70.2	< 0.001
	Europe	4	1.35(0.76-1.94)	< 0.001	71.7	< 0.001

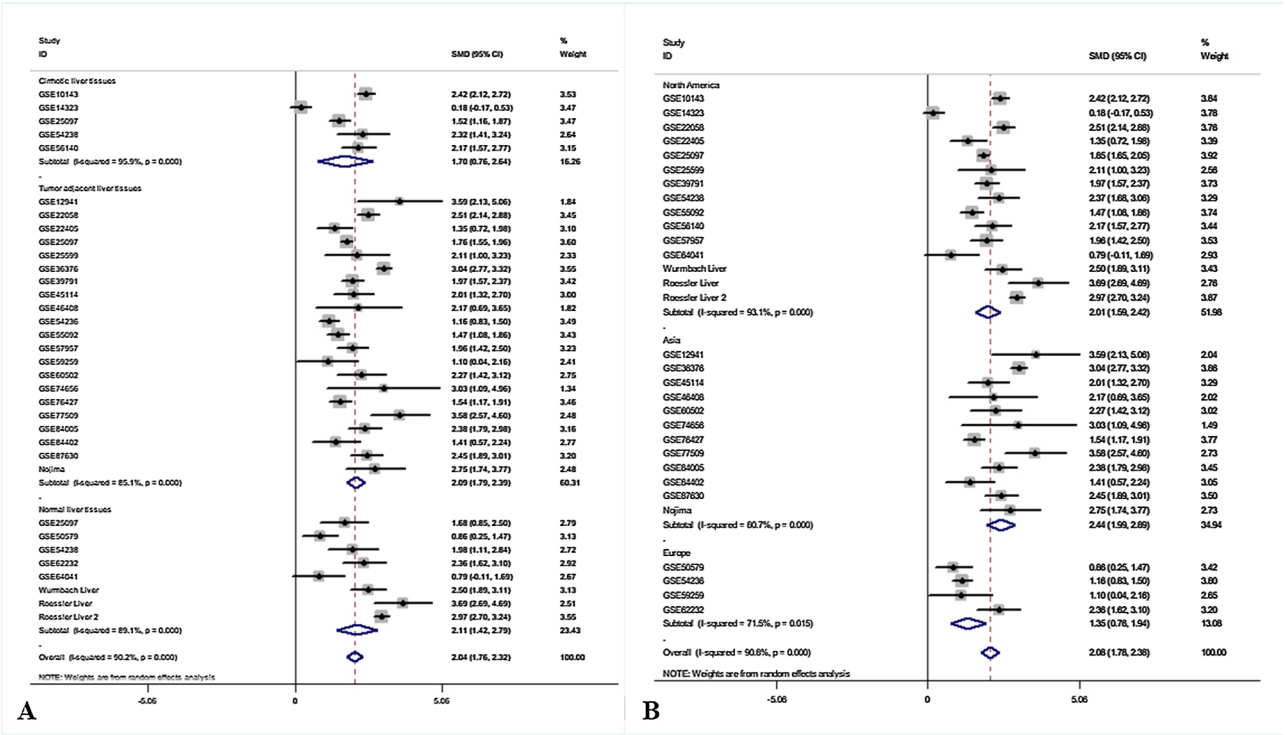

Fig. 8. Subgroup analysis based on control tissue type and the living region of patients. Results showed the control tissue type and the living region of patients were not the source of heterogeneity.

Table 3
Immunohistochemical staining results of CCT3 in cancer and adjacent normal tissues from HPA database.

Patient id	Gender	Age	Tissue	Staining	Quantity	Location	Score
2279	Female	73	Liver cancer	Medium	> 75%	Cytoplasmic/membranous	6
3215	Female	61	Liver cancer	High	> 75%	Cytoplasmic/membranous	9
937	Female	65	Liver cancer	Medium	> 75%	Cytoplasmic/membranous	6
2766	Female	73	Liver cancer	High	> 75%	Cytoplasmic/membranous	9
2177	Female	58	Liver cancer	Low	25%-75%	Cytoplasmic/membranous	2
2578	Male	50	Liver cancer	Medium	> 75%	Cytoplasmic/membranous	6
1163	Male	55	Liver cancer	High	> 75%	Cytoplasmic/membranous	9
2399	Female	52	Liver cancer	Medium	> 75%	Cytoplasmic/membranous	6
2280	Male	80	Liver cancer	High	> 75%	Cytoplasmic/membranous	9
2556	Male	72	Liver cancer	High	> 75%	Cytoplasmic/membranous	9
1252	Female	55	Liver cancer	Medium	25%-75%	Cytoplasmic/membranous	4
282	Female	65	Liver cancer	Medium	> 75%	Cytoplasmic/membranous	6
1720	Male	67	Liver	Medium	< 25%	Cytoplasmic/membranous	2
1846	Female	32	Liver	Medium	< 25%	Cytoplasmic/membranous	2
1899	Female	29	Liver	Medium	< 25%	Cytoplasmic/membranous	2

Table 4
CCT3 expression in liver cancer and adjacent normal tissues.

Group	CCT3		Sum	χ2	P-value
	Negative(%)	Positive(%)			
Liver cancer	1(8.3)	11(91.7)	12	Fisher's Exact Test	0.00879
Adjacent tissues	3(100)	0(0)	3		
Sum	4	11	15		

revealed the mRNA expression of CCT3 was negatively correlated with DNA methylation; this, in turn, indicated that DNA methylation might be one cause of low expression of CCT3 [Fig. 12B].

3.4. Results of Bioinformatics Analysis

RNA-seq counts data from the TCGA database was studied using the edgeR package based on R language. A total of 1,949 differentially expressed genes were obtained, including 1,297 up-regulated genes and 652 down-regulated genes [Fig. 12C]. A total of 10,981 similar genes of CCT3 was found on the MEM website, and 20423 co-expressed genes were found in the cBioPortal database. The results of the GO and KEGG pathways were analyzed base on 858 overlapping genes [Fig. 12D]. The most of the CCT3-relevant genes were related with the GO biological process of "Mitotic sister chromatid segregation", the most significant GO cellular component is "Nuclear chromosome" and the most significant GO molecular function is "Cofactor binding". KEGG signal pathway analysis revealed that "Cell cycle" was the pathway enriched with the majority of CCT3-related genes [Table 7]. A protein–protein interaction network analysis was performed, based on these significant pathways. The results demonstrated the interaction and functional correlation between HCC-related proteins using experimental data, data mined from literature, database data, and results predicted using bioinformatics methods [Fig. 13].

4. Discussion

HCC is the third common cause of tumor death all over the world. As a result of the rising risk of obesity and fatty liver, HCC has become a great challenge to human health. As of yet, there is still no cure for most HCC patients and the development of new drugs is difficult [23]. HCC occurs primarily in the hepatic parenchymal cells. Although we have identified most of the risk factors that might involve in the induction of HCC, the underlying mechanism for the transformation of healthy hepatocytes into tumor cells remains unclear. Various strategies can prevent HCC and improve its clinical treatment, such as controlling alcohol intake, preventing hepatitis B virus (HBV) infection, and ingesting vitamin D and calcium, but we have not yet been able to

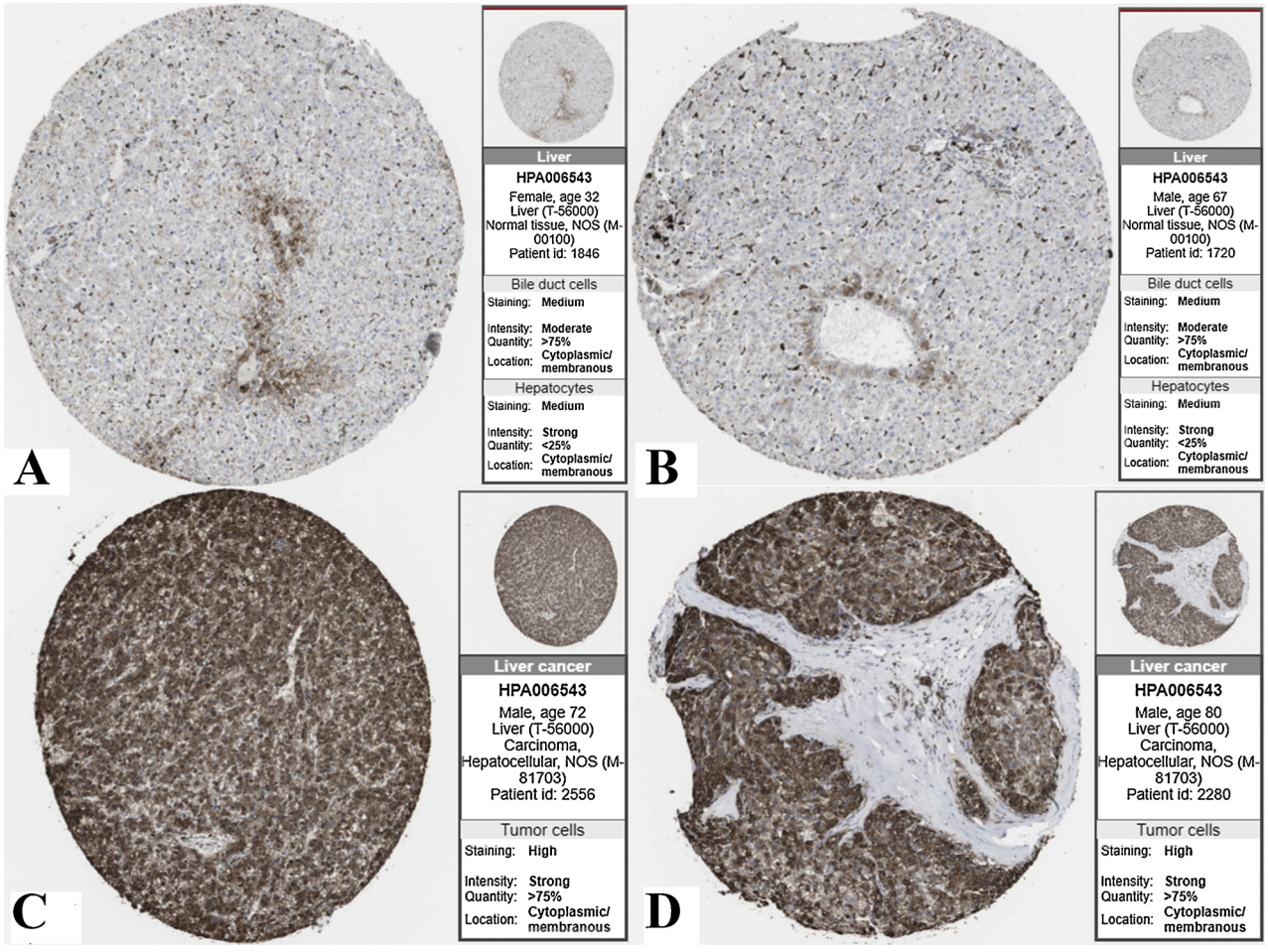

Fig. 9. CCT3 protein expression in normal liver tissues and HCC tissues from the Human Protein Atlas (HPA) database. (A, B) Normal liver tissues stain medium for CCT3, immunohistochemistry, ×100; (C, D) HCC tissues stain high for CDK5, immunohistochemistry, ×100.

Table 5
Relationship between CCT3 expression and clinicopathological parameters.

Parameters		n	Mean value	t value	P value
Tissues	HCC	371	89.320 ± 44.98	25.952	**< 0.001**
	Normal	50	25.390 ± 5.54		
Age	≥60	201	85.390 ± 45.22	−1.777	0.076
	<60	169	93.705 ± 44.38		
Gender	Male	250	91.567 ± 45.38	1.385	0.167
	Female	121	84.676 ± 43.97		
Relative family cancer history	Yes	112	79.680 ± 51.26	−2.794	**0.006**
	No	208	94.253 ± 40.43		
Child-Pugh class	A	217	88.960 ± 45.51	1.037	0.307
	B	21	82.257 ± 26.02		
New tumor event after initial treatment	Yes	95	88.114 ± 42.23	0.176	0.86
	No	174	87.201 ± 39.82		
Neoplasm cancer status	With tumor	110	92.137 ± 55.04	0.812	0.417
	Tumor free	234	87.841 ± 40.70		
Histological grade	G3 ~ G4	134	106.160 ± 45.96	5.538	**< 0.001**
	G1 ~ G2	232	80.059 ± 41.92		
Pathologic stage	III ~ IV	90	92.856 ± 41.59	−0.851	0.395
	I ~ II	257	88.297 ± 44.46		
T stage	T3 ~ T4	93	95.120 ± 48.59	−1.374	0.17
	T1 ~ T2	275	87.711 ± 43.64		
N stage	N1	4	79.012 ± 33.89	−0.6	0.549
	N0	252	91.714 ± 42.12		
M stage	M1	4	107.478 ± 52.12	0.661	0.509
	M0	266	92.302 ± 45.51		
		n	**Mean value**	**F value**	**P value**
Race	Caucasian	184	80.225 ± 44.81	8.276	**< 0.001**
	Asian	158	99.792 ± 44.61		
	African	17	89.281 ± 35.44		

eradicate this disease. The development of this cancer involves multiple signal transduction pathway disorders, gene mutations, and the initiation of inflammatory reactions, which ultimately lead to the formation of tumor blocks [24]. Due to the great harm and complex mechanism of HCC, research on molecular targeted therapy is extremely urgent.

Recently, there has been a growing attention in studying the effect of molecular chaperones in tumor growth. Molecular chaperones have been found over-expressed in many cancer and malignant blood diseases, and been seen as a potential therapeutic target for treatment of malignant tumor [25–27]. Furthermore, molecular chaperones allowing continued cellular proliferation and protein translation, and act as biochemical buffers for many genetic related lesions which may drive tumor occurrence [28].

The t-complex 1 (TCP1) loop complex (TRiC), a certain kind of molecular chaperone, can participate in actin and tubulin folding. CCT is composed of a double-rings structure and each ring contains eight different subunits [29]. Because tubulin and actin are completely dependent on CCT activity to reach natural state, which makes them exclusive substrates for CCT. [30]. The CCT subunit can help complete protein folding and act as a chaperone protein complex [31]. Defects in certain CCT subunits may be more susceptible to certain substrates than changes in other subunits. For instance, in the study reported by Huang et al., knockdown of CCT8 significantly reduced the level of CDK2 in HCC cells [32]. Moreover, Zhang et al documented that CCT1 ~ 5 were over-expressed in HCC tissues and these CCT subunits are all required for cell proliferation as well as proper mitotic progression [39].

CCT3 is also an important subunit in the CCT family. CCT3 can be involved in the tumorigenesis and development of papillary thyroid carcinoma [33], esophageal carcinoma [34], osteosarcomas [35] and gastric cancer [36], its high expression may play key roles in various cancer biological processes. And because CCT3 is also highly expressed in HCC, it may be an important indicator affecting the development of HCC.

RNA expression can be quantified by counting the number of reads mapped to each locus during transcription [37]. These quantitative RNA-Seq read counts were validated with expression chips and qPCR results [38]. Tools that quantify counts are HTSeq, FIXSEQ, Rcount, and Cuffquant [39–43]. The read count is then calculated, and made it suitable for subsequent analysis processing.

In our study, the expression levels of CCT3 in HCC and non-HCC control tissues were extracted from several public databases, including TCGA, GEO, Oncomine, and ArrayExpress, and further statistical analysis was carried out. Based on data obtained from the TCGA database, the difference of CCT3 expression in tumor and non-tumor tissues was compared, and the expression of CCT3 across various clinicopathological parameters was contrasted. It was found that the mRNA and protein levels expression of CCT3 in HCC tissues was higher than those of non-tumor tissues. The expression of CCT3 in other public databases was analyzed and the differential expression of CCT3 in tumor and non-tumor tissues was demonstrated using an SMD forest map and an SROC curve. Analysis of the combined results indicated that CCT3 was highly expressed in HCC tissues and had a high ability to differentiate between cancer tissues and non-cancer tissues. Here, a total of 421 samples from TCGA (HCC, n = 371; non-tumor, n = 50) and 3851 samples from 31 microarray or RNA-sequencing datasets (HCC, n = 1975; non-tumor = 1876) regarding CCT3 in HCC were collected and examined. Meanwhile, clinicopathological parameter data were mined and processed from TCGA database. There were differences in the expression of CCT3 in several clinicopathological parameters, such as race, family history and histological grade. CCT3 was highly expressed in Asian patients, patients with no family history of cancer, and patients with a high pathological grade (G3-G4).

In recent years, research has shown STAT3 could contribute to eukaryotic chaperonin TRiC/CCT biological activity both in vitro and in

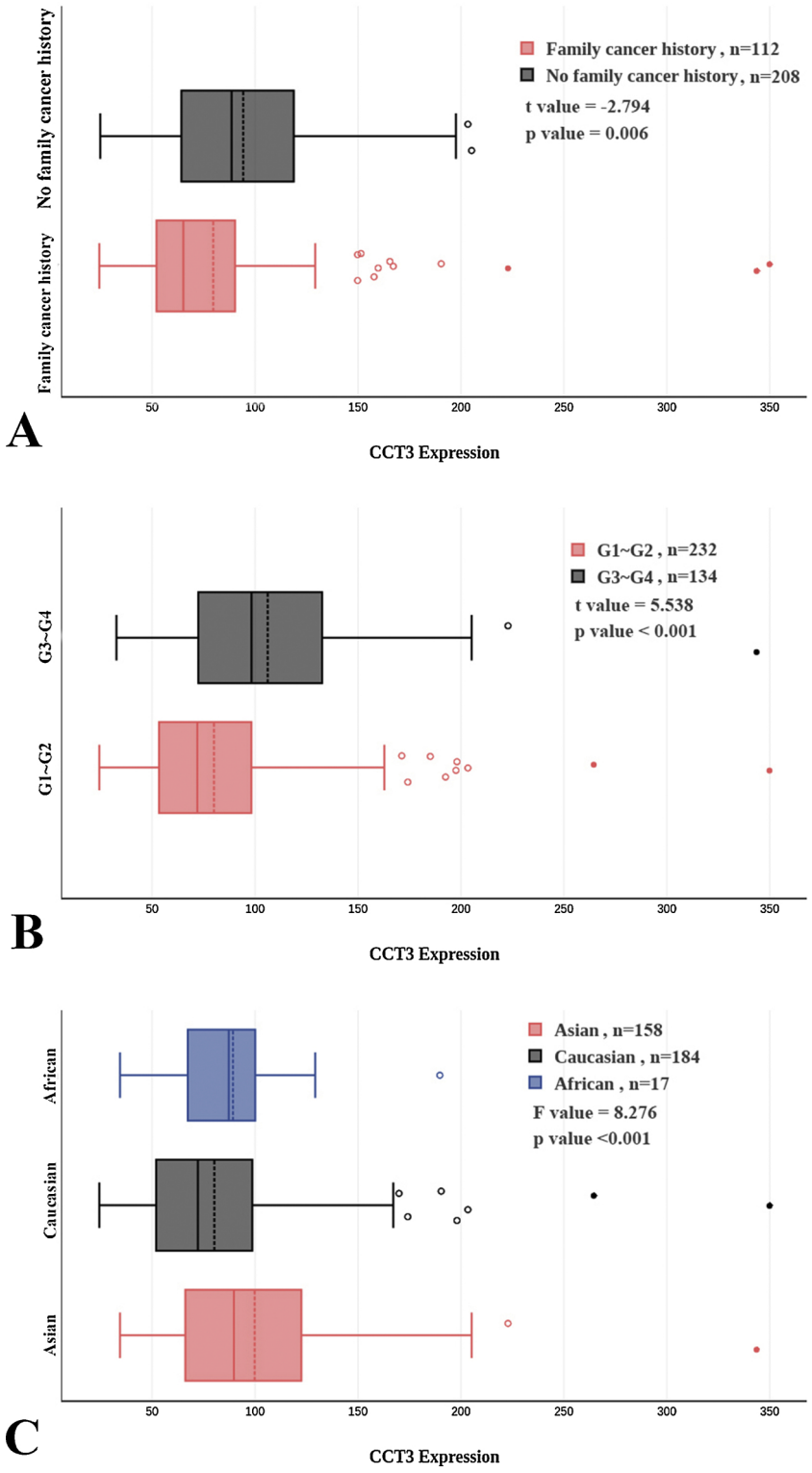

Fig. 10. Clinical value of CCT3 in HCC based on TCGA data. (A) Box chart of CCT3 expression at different relative family cancer histories; (B) Box chart of CCT3 expression at different histological grades; (C) Box chart of CCT3 expression at different races. (CCT3 expression represent the relative expression preprocessed by log-2 transformation.).

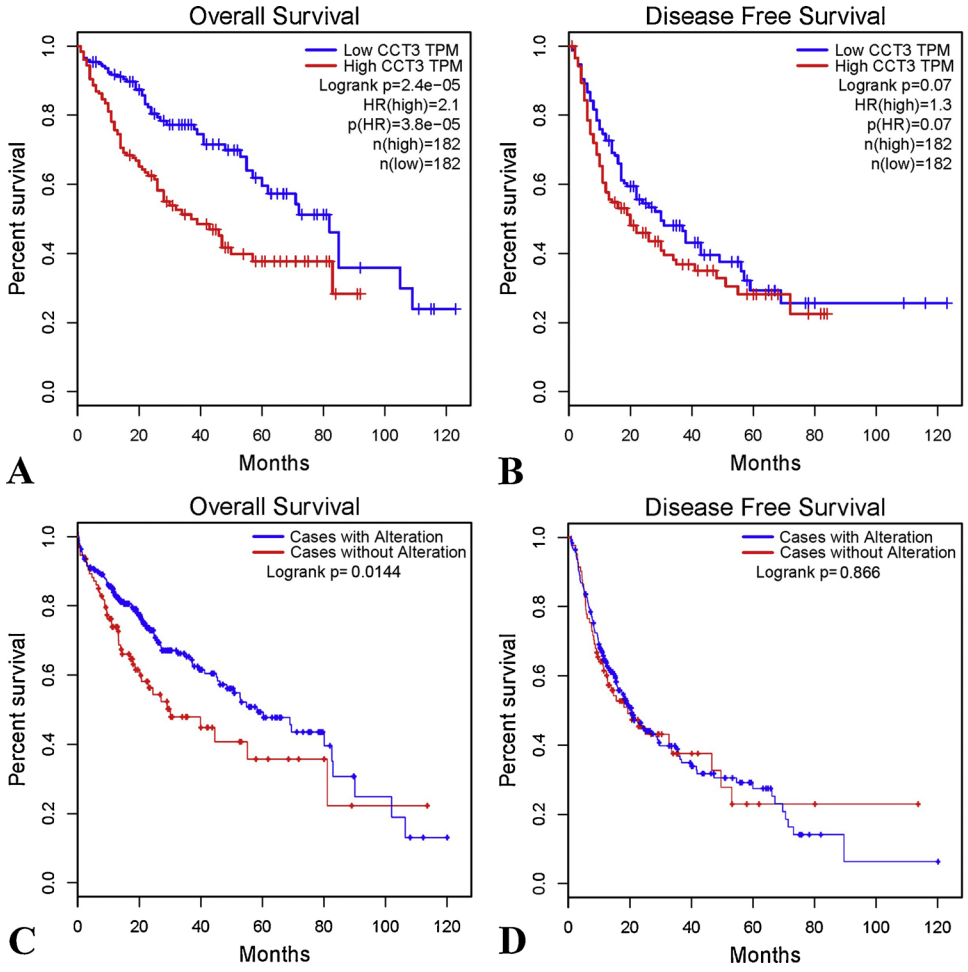

Fig. 11. Prognostic value of CCT3 in HCC based on TCGA data. (A, B) Kaplan-Meier plots revealed an association between increased CCT3 levels and reduced overall survival; (C, D) Kaplan-Meier plots revealed an association between CCT3 amplification and reduced overall survival.

vivo. TRiC binding to STAT3 was mediated by TRiC subunit CCT3 [44]. STAT3 is a key transcription factor in the IL-6/STAT3 signaling pathway and its activated form can enter the nuclei of cancer cells in HCC [45]. When stimulated with IL-6, Cui et al found STAT were significantly down-regulated in the CCT3-siRNA HCC cell lines. Therefore, CCT3 may play an important role in the translocation of and STAT3 from the cytoplasm into the nuclei. This study explain the association between the over-expression of CCT3 in the cancer cell nucleus with the progression of HCC, and why CCT3 may be a key target that affects the activity of STAT3 in HCC [18].

Furthermore, a previous study designed by Zhang et al was performed to detect moderate or low-frequency mutated cancer driver genes in HCC, and integrated analyses were conducted on these novel cancer driver genes. Two genes, transportin 1 (TNPO1) and CCT3, were hypomethylated and over-expressed, and high expression of TNPO1 and CCT3 indicated a poor prognosis in HCC patients [46]. In a study based on bioinformatics methods conducted by Wang et al, the results of real time PCR and TCGA database proof validation that 10 genes (including CCT3) were differently expressed in HCC and healthy liver tissues. Among these ten genes, only the expression of CCT3 and other two genes showed association with OS of HCC patients in TCGA database ($P < 0.05$) [47]. Also, according to the paper written by Zhang et al, CCT3 may play a role in regulating microtubule structure and function, they boldly predict that CCT3 may affect the sensitivity to microtubule targeting agents. Thus, CCT3 may be a potential therapeutic drug target for HCC and other cancers treated with microtubule-destabilizing drug, and improve the drug sensitivity [48]. These are the mechanisms that CCT3 might play a role in HCC tumor progression.

In our research, we also focus on exploring the molecular mechanisms by which CCT3 may be involved in HCC. By searching for the differentially expressed genes related to HCC in the TCGA database and overlapping with the co-expressed similar genes of CCT3, the differentially expressed genes related to CCT3 in the HCC mRNA expression profile were screened out. A total of 858 differentially expressed genes were analyzed by GO and KEGG pathway, and protein interaction networks were drawn to explore the means by which CCT3 affects the occurrence and development of HCC. Gene Ontology is an ontology widely used in the field of bioinformatics. It covers three most important aspects of biology: cellular component, molecular function and biological process. For a group of proteins or RNA, GO can use certain terms to describe their function or where they are located or which biological process they are involved in. The majority of the CCT3-relevant genes were significantly represented by the GO biological

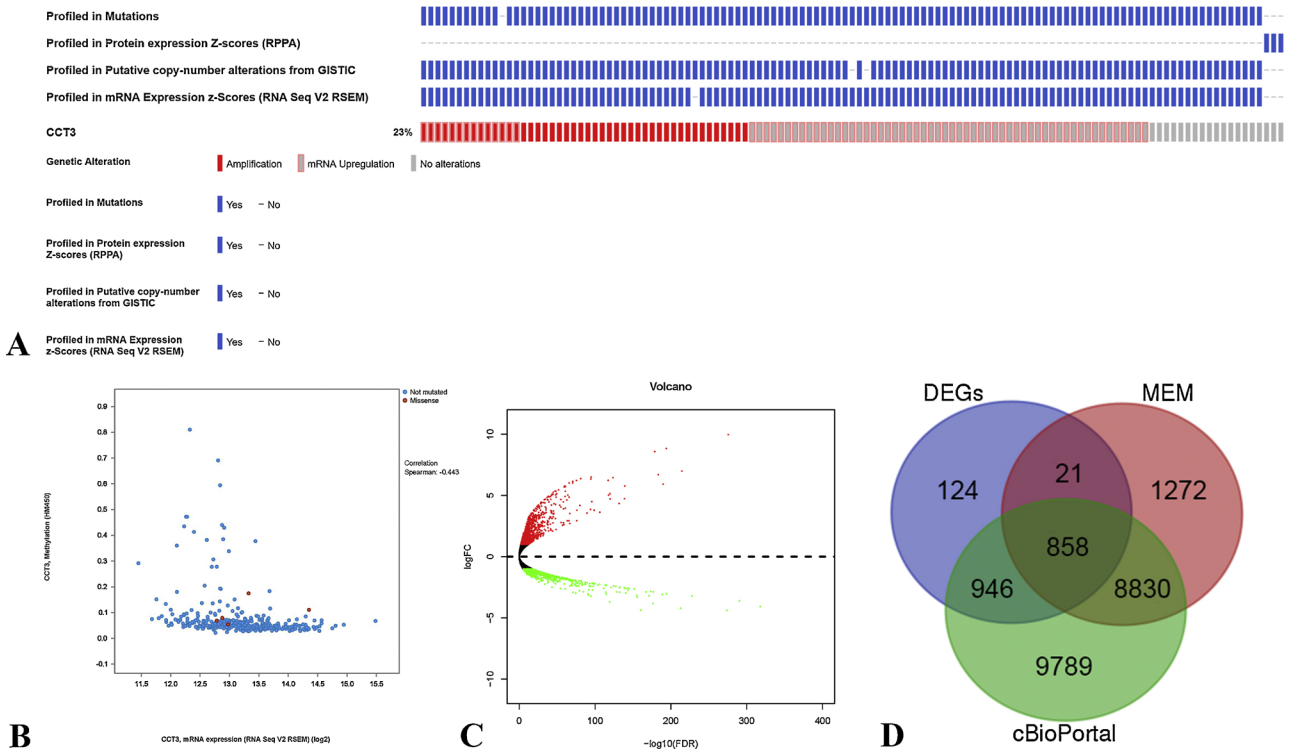

Fig. 12. CCT3 genetic alteration from cBioPortal and identification of CCT3-related genes. (A) Genetic alteration of CCT3 in HCC patients, based on the cBioPortal database; Gene alteration of CCT3 in HCC. The OncoPrint schematic showed that gene alteration of CCT3 occurred in 102 (23%) of all 440 sequenced patients, including 55 patients of mRNA up-regulation, 32 patients of amplification, and 14 patients of mixed type of amplification and mRNA up-regulation (we have omitted part of the "No alteration" half of this picture); (B) Spearman analyse was conducted. The correlation coefficient is -0.443, suggested the mRNA expression of CCT3 was negatively correlated with DNA methylation; (C) Volcano plot of differentially expressed genes (DEGs) between HCC and non-HCC tissues based on TCGA dataset. Red points indicate high expression, while green points represent low expression. (D) Venn diagram for intersection gene screening.

Table 6
Mutation types of CCT3 in HCC patients from COSMIC.

Position	Mutation	Mutation (Amino Acid)	Mutation ID (COSM)	Count	Mutation Type
85	c.254 G > C	p.R85P	COSM4930130	1	Substitution – Missense
138	c.413 A > G	p.K138R	COSM4622156	1	Substitution – Missense
155	c.464 T > A	p.I155N	COSM5041673	1	Substitution – Missense
282	c.845 T > A	p.I282N	COSM4942614	1	Substitution – Missense
287	c.859C > T	p.P287S	COSM4939742	1	Substitution – Missense
322	c.965 G > T	p.R322L	COSM328681	1	Substitution – Missense
384	c.1150C > A	p.L384I	COSM4802547	2	Substitution – Missense
398	c.1193 G > T	p.C398F	COSM5038963	1	Substitution – Missense
399	c.1196 G > A	p.R399H	COSM4917367	1	Substitution – Missense
424	c.1270 G > A	p.E424K	COSM5042218	1	Substitution – Missense

process of “Mitotic sister chromatid segregation”, the most significant GO cellular component is “Nuclear chromosome” and the most significant GO molecular function is “Cofactor binding”. The abnormality of chromatid separation in mitotic sisters, that is, the instability of nuclear chromosomes is closely related to the occurrence and development of tumors. Cofactor binding promotes the progression of most biological activities, and can also affect the regulation of a variety of tumor-related signaling pathways. In addition, KEGG pathway analysis revealed that “Cell cycle” was the most important pathway related with CCT3-related genes. Tumors are a type of cell cycle disease. The cell cycle changes under the influence of gene regulation, eventually leading to tumorigenesis. At the same time, we can also rely on this type of mechanism to study molecular treatment methods against malignant tumors. DNA methylation is an important epigenetic modification, and epigenetic changes are one of the most important features of cell carcinogenesis. The level of methylation means the silencing and activation of genes, and changes in the level of DNA methylation can lead to tumorigenesis or abnormal proliferation of tumor cells through various pathways. Through the analysis of the epigenetic data provided by the TCGA database, we found that the mRNA expression of CCT3 in HCC was negatively correlated with DNA methylation. These are the basis for our in-depth analysis of the potential mechanism of action of CCT3 in HCC.

Overall, a few studies had demonstrated the significant role of CCT3 in the development and progression of HCC. However, none of these studies conducted large-scale databases mining or meta-analysis to verify their conclusions. In our study, we paid more attention to investigating the potential diagnostic and prognostic value of CCT3. Thus,

Table 7
Top five significant pathways of GO and KEGG terms.

Category	Term	PValue	FDR	Top 5 Genes
GOTERM_BP_DIRECT	GO:0000070 Mitotic sister chromatid segregation	0	0	SMC4;NDC80;TACC3;CENPA;SPAG5;
GOTERM_BP_DIRECT	GO:0000278 Mitotic cell cycle	0	0	SMC4;KIF20 A;SPRY2;CDKN2 A;CDKN2C;
GOTERM_BP_DIRECT	GO:0000280 Nuclear division	0	0	SMC4;NDC80;TACC3;CENPA;P3H4;
GOTERM_BP_DIRECT	GO:0000819 Sister chromatid segregation	0	0	SMC4;NDC80;TACC3;CENPA;SPAG5;
GOTERM_BP_DIRECT	GO:0006260 DNA replication	0	0	CHAF1 A;RNASEH2 A;EHMT2;CHEK1;RMI2;
GOTERM_CC_DIRECT	GO:0000228 Nuclear chromosome	0	0	CHAF1 A;CITED2;NDC80;CENPA;P3H4;
GOTERM_CC_DIRECT	GO:0000775 Chromosome, centromeric region	0	0	NDC80;CENPA;SPAG5;CENPF;KIF2C;
GOTERM_CC_DIRECT	GO:0000779 Condensed chromosome, centromeric region	0	0	NDC80;CENPA;SPAG5;CENPF;KIF2C;
GOTERM_CC_DIRECT	GO:0000793 Condensed chromosome	0	0	SMC4;NDC80;CENPA;P3H4;SPAG5;
GOTERM_CC_DIRECT	GO:0005694 Chromosome	0	0	CHAF1 A;SMC4;CDKN2 A;CITED2;NDC80;
GOTERM_MF_DIRECT	GO:0048037 Cofactor binding	2.64E-12	4.83E-09	DHODH;ABAT;ALAS1;ETFDH;ALB;
GOTERM_MF_DIRECT	GO:0050662 Coenzyme binding	1.25E-10	1.14E-07	ETFDH;FASN;FMO3;G6PD;PHGDH;
GOTERM_MF_DIRECT	GO:0032553 Ribonucleotide binding	5.70E-10	2.21E-07	GNE;SMC4;ABCC5;KIF20 A;DDX39 A;
GOTERM_MF_DIRECT	GO:0032550 Purine ribonucleotide binding	6.75E-10	2.21E-07	GNE;SMC4;ABCC5;KIF20 A;DDX39 A;
GOTERM_MF_DIRECT	GO:0001883 Purine nucleoside binding	7.52E-10	2.21E-07	GNE;SMC4;ABCC5;KIF20 A;DDX39 A;
KEGG_PATHWAY	hsa04110 Cell cycle	1.29E-14	3.90E-12	CDKN2 A;CDKN2C;CHEK1;SFN;MAD2L1;
KEGG_PATHWAY	hsa03030 DNA replication	4.32E-11	6.54E-09	RNASEH2 A;FEN1;POLA2;LIG1;MCM2;
KEGG_PATHWAY	hsa00280 Valine, leucine and isoleucine degradation	6.87E-09	6.94E-07	DBT;ABAT;ECHS1;EHHADH;ALDH2;
KEGG_PATHWAY	hsa01100 Metabolic pathways	1.21E-07	7.49E-06	GNE;NAMPT;GPHN;CDS1;PEMT;
KEGG_PATHWAY	hsa00640 Propanoate metabolism	1.24E-07	7.49E-06	DBT;ABAT;ECHS1;EHHADH;MLYCD;

the large-scale sample size of our research indicated high credibility of our integrated analysis of gene expression datasets. We are the first to use a variety of mining methods to collect data (such as microarray, RNA sequencing, literature and immunohistochemistry data), comprehensive analysis of the clinical and prognostic significance of CCT3 in HCC. At the same time, we used a variety of meta-analytic methods, including SMD forest maps, sensitivity analysis, subgroup analysis and sROC curves, to verify the final results. We also further explained the potential mechanism of CCT3 in HCC through GO and KEGG signal pathway analysis and PPI analysis. The most important KEGG pathway related with CCT3-related genes is “Cell cycle”. Many studies have confirmed that cell cycle changes or molecular drug intervention in the cell cycle can affect the occurrence and development of HCC [49,50]. At the same time, by PPI analysis of CCT3-related genes enriched in KEGG signaling pathways, we found five genes that are most relevant to other genes (connected nodes greater than 24): CDK1, PCNA, CCNA2, CHEK1 and CCNB1. CDK1 exhibited high expression in HCC cells and can promote tumor cell proliferation via cell cycle pathway [51]. Strong and diffuse nuclear PCNA immunoreactivity was observed in HCC tissues. PCNA showed unique immunostaining characteristics in HCCs, which can be useful a marker to aid in the distinction of HCC from benign liver nodular lesions [52]. CCNA2 can perform an intermediary role between the HCV viral proteins and the dysfunctional module in the HCV key genes interaction network and provided valuable information for understanding the mechanism of HCV-induced HCC progression [53].Previous studies reported that CHEK1 was over-expressed in HCC and associated with poor prognosis [54]. The high level expression of CCNB1 is closely associated with poor prognosis in HCC patients [55]. These genes play an important role in the biological process of HCC, indicating that CCT3 may regulate HCC by targeting related sites and gene enrichment pathways.

However, our research still has some limitations. Because HPA database only provides two cases of normal liver immunohistochemistry result, our validation of differential expression of CCT3 at the protein level is not sufficient. Although the GO and KEGG signaling pathways, as well as PPI analysis were performed in our study, we still haven’t carried out sufficient mechanism analysis for CCT3 in the pathogenesis and development of HCC. In addition, we haven’t performed the CCT3 relevant in vivo and in vitro experiments, these will continue to conduct in-depth research in our subsequent study.

In summary, this study carries out the staging and prognostic analysis of HCC. It suggests that CCT3 might play an important role in the tumorigenesis and progression of HCC and may have a certain prognostic value in HCC. CCT3 might represent a promising biomarker for HCC. However, functional and medication experiments are still required to discover the molecular mechanism of CCT3 in HCC.

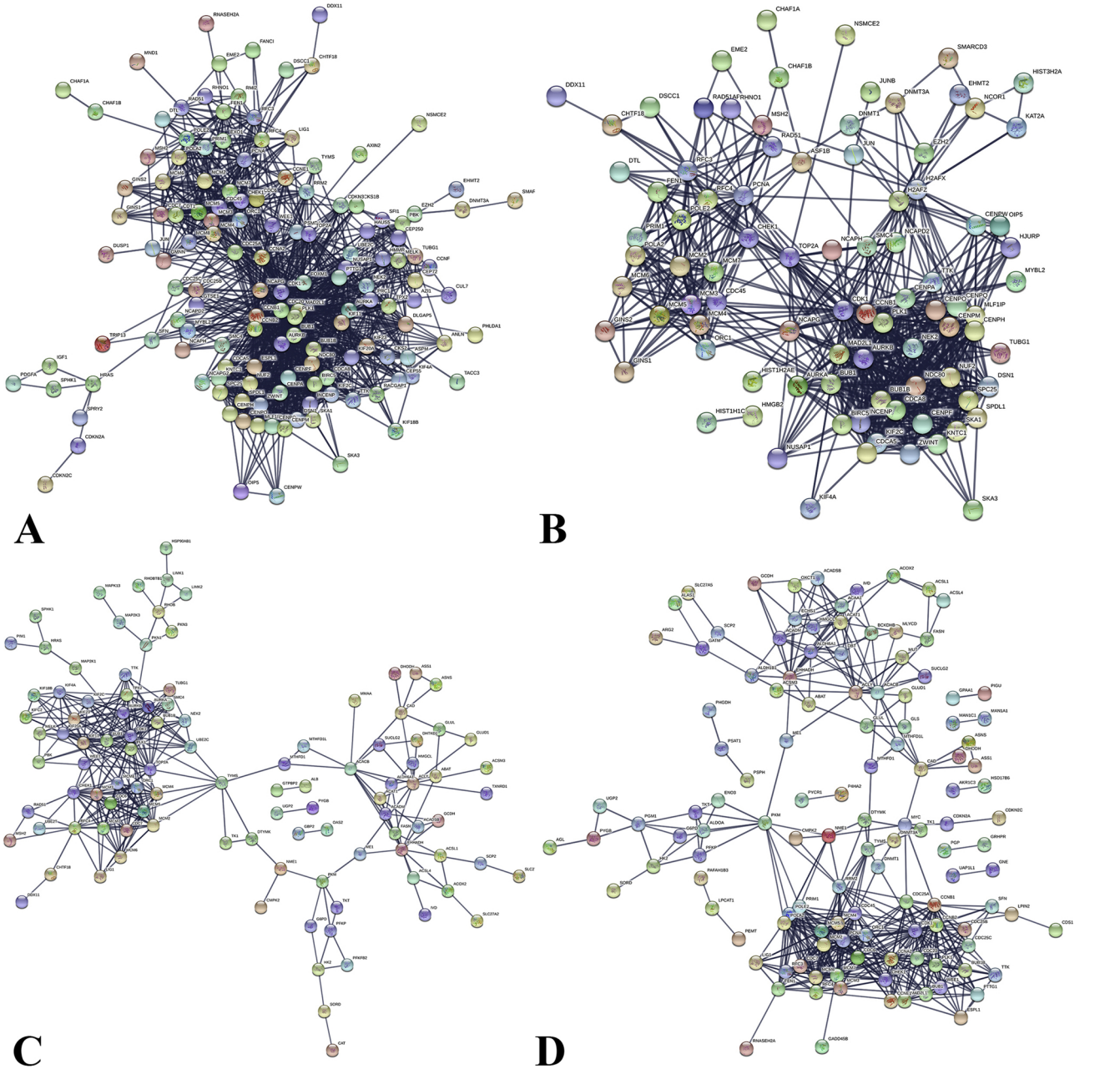

Fig. 13. Protein–protein interactions of enriched gene on the top five GO and KEGG pathways. The the thickness of lines indicates the strength of data support. Disconnected nodes are hidden in this network. (A) biological process; (B) cellular component; (C) molecular function; (D) KEGG.

Conflict of interests

The authors declare that no competing interest exists.

Acknowledgements

This work was supported by a Medical Excellence Award funded by a Creative Research Development Grant from the First Affiliated Hospital of Guangxi Medical University.

References

[1] R.L. Siegel, K.D. Miller, A. Jemal, Cancer statistics, CA Cancer J. Clin. 68 (2018) 7–30.
[2] D. Sia, A. Villanueva, S.L. Friedman, et al., Liver cancer cell of origin, molecular class, and effects on patient prognosis, Gastroenterology 152 (2016) 745.
[3] C.K. Yang, T.D. Yu, C.Y. Han, et al., Genome-wide association study of MKI67 expression and its clinical implications in HBV-related hepatocellular carcinoma in southern China, Cell. Physiol. Biochem. 42 (2017) 1342–1357.
[4] C. Ye, R. Tao, Q. Cao, et al., Whole-genome DNA methylation and hydroxymethylation profiling for HBV-related hepatocellular carcinoma, Int. J. Oncol. 49 (2016) 589.
[5] X.P. Zhang, K. Wang, N. Li, et al., Survival benefit of hepatic resection versus transarterial chemoembolization for hepatocellular carcinoma with portal vein tumor thrombus: a systematic review and meta-analysis, BMC Cancer 17 (2017) 902.
[6] D. Kaemmerer, R. Schindler, F. Mußbach, et al., Somatostatin and CXCR4 chemokine receptor expression in hepatocellular and cholangiocellular carcinomas: tumor capillaries as promising targets, BMC Cancer 17 (2017) 896.
[7] Q. Zhu, M. Luo, C. Zhou, et al., A proteomics-based investigation on the anticancer activity of alisertib, an Aurora kinase A inhibitor, in hepatocellular carcinoma Hep3B cells, Am. J. Transl. Res. 9 (2017) 3558–3572.
[8] C.M. Chiu, S.Y. Huang, S.F. Chang, et al., Synergistic antitumor effects of tanshinone IIA and sorafenib or its derivative SC-1 in hepatocellular carcinoma cells, Oncol. Ther. 11 (2018) 1777–1785.
[9] P. Intaraprasong, S. Siramolpiwat, R.K. Vilaichone, Advances in management of hepatocellular carcinoma, Asian Pac J Cancer. 17 (2016) 3697.
[10] N.M. Tunissiolli, M.M. Castanhole-Nunes, P.R. Biselli-Chicote, et al., Hepatocellular

carcinoma: a comprehensive review of biomarkers, clinical aspects, and therapy, Asian Pac J Cancer. 18 (2017) 863.
[11] Q. Pang, H. Jin, K. Qu, et al., The effects of nonsteroidal anti-inflammatory drugs in the incident and recurrent risk of hepatocellular carcinoma: a meta-analysis, Onco. Ther. 10 (2017) 4645–4656.
[12] J. Zucman-Rossi, A. Villanueva, J.C. Nault, et al., Genetic landscape and biomarkers of hepatocellular carcinoma, Gastroenterology. 149 (2015) 1226–1239 e4.
[13] H. Kubota, G. Hynes, A. Carne, et al., Identification of six TCP-1-related genes encoding divergent subunits of the TCP-1-containing chaperonin, Curr. Biol. 4 (1994) 89–99.
[14] N.A. Walkley, A.G. Demaine, A.N. Malik, Cloning, structure and mRNA expression of human CCTG, which encodes the chaperonin subunit CCT gamma, Biochem. J. 313 (1996) 381.
[15] F. Wang, R. Wang, Q. Li, et al., A transcriptome profile in hepatocellular carcinomas based on integrated analysis of microarray studies, Diagn. Pathol. 12 (2017) 4.
[16] N. Wong, A. Chan, S.W. Lee, et al., Positional mapping for amplified DNA sequences on 1q21-q22 in hepatocellular carcinoma indicates candidate genes over-expression, J. Hepatol. 38 (2003) 298–306.
[17] E.N. Qian, S.Y. Han, S.Z. Ding, et al., Expression and diagnostic value of CCT3 and IQGAP3 in hepatocellular carcinoma, Cancer Cell Int. 16 (2016) 1–8.
[18] X. Cui, Z.P. Hu, Z. Li, et al., Overexpression of chaperonin containing TCP1, subunit 3predicts poor prognosis in hepatocellular carcinoma, World J. Gastroenterol. 21 (2015) 8588–8604.
[19] Y. Zhang, Y. Wang, Y. Wei, et al., Molecular chaperone CCT3 supports proper mitotic progression and cell proliferation in hepatocellular carcinoma cells, Cancer Lett. 372 (2015) 101–109.
[20] R. Zhang, P. Lin, H. Yang, et al., Clinical role and biological function of CDK5 in hepatocellular carcinoma: a study based on immunohistochemistry, RNA-seq and in vitro investigation, Oncotarget 8 (2017) 108333–108354.
[21] G.P. Wagner, K. Kin, V.J. Lynch, Measurement of mRNA abundance using RNA-seq data: RPKM measure is inconsistent among samples, Theory Biosci. 131 (2012) 281–285.
[22] M.D. Robinson, D.J. McCarthy, G.K. SmythK, EdgeR: a Bioconductor package for differential expression analysis of digital gene expression data, Bioinformatics 26 (2010) 139–140.
[23] A. Gerbes, F. Zoulim, H. Tilg, et al., Gut roundtable meeting paper: selected recent advances in hepatocellular carcinoma, Gut. 67 (2018) gutjnl-2017-315068.
[24] R. Dutta, R.I. Mahato, Recent advances in hepatocellular carcinoma therapy, Pharmacol. Therapeut. (2017).
[25] Y. Lin, W. Tsai, H. Liu, et al., Intracellular beta-tubulin/chaperonin containing TCP1-beta complex serves as a novel chemotherapeutic target against drug-resistant tumors, Cancer Res. 69 (2009) 6879–6888.
[26] K. Sankhala, M. Mita, A. Mita, et al., Heat shock proteins: a potential anticancer target, Drug Targets. 12 (2011) 2001–2008.
[27] H. Reikvam, E. Ersvaer, O. Bruserud, Heat shock protein 90 – a potential target in the treatment of human acute myelogenous leukemia, Cancer Drug Targets. 9 (2009) 761–776.
[28] F. Koga, K. Kihara, L. Neckers, Inhibition of cancer invasion and metastasis by targeting the molecular chaperone heat-shock protein 90, Anticancer Res. 29 (2009) 797–807.
[29] M. Chagoyen, L. Carrascosa, Molecular determinants of the ATP hydrolysis asymmetry of the CCT chaperonin complex, Proteins Struct. Funct. Bioinform. 82 (2014) 703–707.
[30] R. Willison, The substrate specificity of eukaryotic cytosolic chaperonin CCT, Philos. Trans. R. Soc. Lond., B, Biol. Sci. 373 (2018) 20170192.
[31] T. Lopez, K. Dalton, J. Frydman, The mechanism and function of group II chaperonins, J. Mol. Biol. 427 (2015) 2919–2930.
[32] X. Huang, X. Wang, C. Cheng, et al., Chaperonin containing TCP1, subunit 8 (CCT8) is upregulated in hepatocellular carcinoma and promotes HCC proliferation, APMIS 122 (2014) 1070–1079.
[33] X. Shi, S. Cheng, W. Wang, Suppression of CCT3 inhibits malignant proliferation of human papillary thyroid carcinoma cell, Oncol. Lett. 15 (2018) 9202.
[34] P. Su, S. Wen, Y. Zhang, et al., Identification of the key genes and pathways in esophageal carcinoma, Gastroenterol. Res. Pract. (2016) 2968106.
[35] Y. Xiong, S. Wu, Q. Du, et al., Integrated analysis of gene expression and genomic aberration data in osteosarcoma (OS), Cancer Gene Ther. 22 (2015) 524–529.
[36] L.J. Li, L.S. Zhang, Z.J. Han, et al., Chaperonin containing TCP-1 subunit 3 is critical for gastric cancer growth, Oncotarget 8 (2017) 111470–111481.
[37] M. Griffith, J.R. Walker, N.C. Spies, Informatics for RNA sequencing: a web resource for analysis on the cloud, PLoS Comput. Biol. 11 (2015) e1004393.
[38] M. Kasembeli, W. Lau, S. Roh, et al., Modulation of STAT3 folding and function by TRiC/CCT chaperonin, PLoS Biol. 12 (2014) e1001844.
[39] S. Anders, P.T. Pyl, W. Huber, HTSeq–a Python framework to work with high-throughput sequencing data, Bioinformatics 31 (2015) 166–169.
[40] Y. Liao, G.K. Smyth, W. Shi, featureCounts: an efficient general purpose program for assigning sequence reads to genomic features, Bioinformatics 30 (2014) 923–930.
[41] M.W. Schmid, U. Grossniklaus, Rcount: simple and flexible RNA-Seq read counting, Bioinformatics 31 (2015) 436–437.
[42] F. Finotello, E. Lavezzo, L. Bianco, Reducing bias in RNA sequencing data: a novel approach to compute counts, BMC Bioinformatics 15 (2014) S7.
[43] T.B. Hashimoto, M.D. Edwards, D.K. Gifford, Universal count correction for high-throughput sequencing, PLoS Comput. Biol. 10 (2014) e1003494.
[44] Z.H. Zhang, D.J. Jhaveri, V.M. Marshall, A comparative study of techniques for differential expression analysis on RNA-Seq data, PLoS One 9 (2014) e103207.
[45] W.C. Li, S.L. Ye, R.X. Sun, et al., Inhibition of growth and metastasis of human hepatocellular carcinoma by antisense oligonucleotide targeting signal transducer and activator of transcription 3, Clin. Cancer Res. 12 (2006) 7140–7148.
[46] Z. Zhang, L. Xu, C. Sun, Comprehensive characterization of cancer genes in hepatocellular carcinoma genomes, Oncol. Lett. 15 (2018) 1503–1510.
[47] F. Wang, R. Wang, Q. Li, et al., A transcriptome profile in hepatocellular carcinomas based on integrated analysis of microarray studies, Diagn. Pathol. 12 (2017) 4.
[48] Y. Zhang, Y. Wang, Y. Wei, et al., Molecular chaperone CCT3 supports proper mitotic progression and cell proliferation in hepatocellular carcinoma cells, Cancer Lett. 372 (2016) 101–109.
[49] Z. Liu, J. Li, J. Chen, et al., MCM family in HCC: MCM6 indicates adverse tumor features and poor outcomes and promotes S/G2 cell cycle progression, BMC Cancer 18 (2018) 200.
[50] C. Yang, A. Hou, C. Yu, et al., Kanglaite reverses multidrug resistance of HCC by inducing apoptosis and cell cycle arrest via PI3K/AKT pathway, Onco. Ther. 11 (2018) 983–996.
[51] C.L. Gao, G.W. Wang, G.Q. Yang, et al., Karyopherin subunit-α 2 expression accelerates cell cycle progression by upregulating CCNB2 and CDK1 in hepatocellular carcinoma, Oncol. Lett. 15 (2018) 2815–2820.
[52] J.P. Lai, Z.M. Chen, T. Lok, et al., Immunohistochemical stains of proliferating cell nuclear antigen, insulin-like growth factor 2 and clusterin help distinguish malignant from benign liver nodular lesions, J. Clin. Pathol. 67 (2014) 464–469.
[53] G. Bai, W. Zheng, W. Ma, Identification and functional analysis of a core gene module associated with hepatitis C virus-induced human hepatocellular carcinoma progression, Oncol. Lett. 15 (2018) 6815–6824.
[54] J. Yang, Z. Hou, C. Wang, et al., Gene expression microarray analysis reveals prognostic markers of survival in high grade astrocytomas, Neurol. Res. 15 (2018) 1–8.
[55] N. Chai, H.H. Xie, J.P. Yin, et al., FOXM1 promotes proliferation in human hepatocellular carcinoma cells by transcriptional activation of CCNB1, Biochem. Biophys. Res. Commun. 500 (2018) 924–929.